Assessing Passive In Situ Reactive Media Hydraulics by Direct Velocity Measurements In the Laboratory and Field

By

Allison M. Cormican
B.Sc., Southwest Baptist University, 2018

Submitted to the graduate degree program in Geology and the Graduate Faculty of the University of Kansas in partial fulfillment of the requirements for the degree of Master of Science.

Chair: J. F. Devlin

Mary C. Hill

Andrea E. Brookfield

Date Defended: 5 June 2020

The thesis committee for Allison M. Cormican certifies that this is the approved version of the following thesis:

Assessing Passive In Situ Reactive Media Hydraulics by Direct Velocity Measurements In the Laboratory and Field

_____

Chair: J. F. Devlin

Date Approved: 5 June 2020

Abstract

A Horizontal Reactive Media Treatment Well (HRX Well) is a novel groundwater remediation technology, which comprises a horizontal well filled with reactive media. Point Velocity Probes (PVPs) were installed in a pilot HRX Well system for treatment of trichloroethene in a silty-sandy aquifer at Vandenburg Air Force Base. The PVPs supported evaluations of the HRX Well hydraulic performance. The PVP design and reactive porous medium were customized for the site. First, hydraulic conductivities (K) of reactive treatment media mixtures were measured in the laboratory using grain size analysis methods, permeametry, and a field scale column test (comparable in size to an HRX Well cartridge). Sixteen grain size algorithms were used to estimate K. The USBR, Slichter, and Shepherd methods, applied to a variety of iron and sand mixtures, agreed well with permeametry and field scale column, producing K estimates that fell within 30 and 60 m/d. The shape, length, and width of the prototype PVP probes did not affect the accuracy of velocity measurements, compared to ±20% differences in porosity between packings. However, two-dimensional (2-D) modeling indicated that a probe occupying more than 16% of the cartridge/column cross-sectional area would cause measurable effects on seepage velocity. Field trials involving the PVPs resulted in accurate seepage velocities measured in the HRX Well, as indicated by 2-D and three-dimensional (3-D) modeling. In addition to supporting the HRX technology, the work performed in this thesis contributed to the broader scientific issues of scaling hydraulic properties measurements from the laboratory to the field of engineered porous media, elucidating hydraulic properties of mixed porous media, simplifying 3-D flow systems to 2-D in radial and cartesian coordinates, and demonstrating direct effects on seepage velocity by desaturation of sandy porous media.

Acknowledgements

First of all, I would like to thank my advisor, Dr. Rick Devlin, for his guidance and mentorship through the research development and writing. Thank you for providing me with the opportunity to start on the research team that first summer. Not only are you the great teacher, not also I really appreciate your genuine and friendly nature that makes the work environment fun. I would also like to thank my committee members, Dr. Mary C. Hill and Dr. Andrea E. Brookfield, for their many insights and hours of paper editing. I want to give a huge thank you to Trevor Osorno for helping so much in the laboratory, whether is be soldering PVPs or 3D printer training. Your excitement for laboratory work is contagious. Thank you to Bryan Heyer, Matt Jones, and Billy Hodge for your help as well in the laboratory and writing process.

Several other people involved in the work for the first field-scale HRX Well implementation deserve recognition. Thank you, Dr. Craig Divine from Arcadis, for your help with modeling evaluation and reviewing during the writing process. Thank you to Jesse Wright from Arcadis for help with field data collection. Thank also to Dr. Michelle Crimi and Blossom Nzeribe from Clarkson University for help with laboratory column experiments.

I would like to thank my Biology professors at my undergraduate university, Southwest Baptist University, for preparing me for the next step of graduate school. Additionally, I would like to say a special thank you to my fiancé, Jacob Immel, for your support through this process of obtaining my Masters, whether that be running through a presentation together or taking a much-needed mental break to grab some ice cream. Thank you also to the friends and family who supported me through this process. Thanks, mom and dad, for helping me get to this point. I wouldn't be here without your help. Lastly, I would like to thank God for blessing me with this opportunity and giving me strength to persevere through the process.

Table of Contents

List of Figures

Figure 3.1: (a) Peristaltic pump recirculating flow from (b) a 10 L reservoir through a PVP Column filled with (c) porous media. (d) the detector array consisting of a tracer injection port and two detector wires. Arrows indicate the pathway of water flow within the closed system.

Figure 3.2: A) Grain size distribution of medium sand used in this work and that reported by Li et al. (2013). B) Drainage and imbibition curves for the sand modified from Li et al., (2013).

Figure 3.3: Schematic diagram of a passively operated HRX Well showing the location of the sand-packed PVP cartridges placed to monitor flow into and out of the closed treatment section of the well. Contaminated water enters the intake screen, and treated water exits through the outlet screen. Additional details are given in Divine et al. (2020).

Figure 3.4: Effect of PVP diameter on measurement accuracy. Simple Darcy calculations (Darcy *v*) and selected PVP radii in a radial finite difference flow model (F.D. Model *v*) show the measured velocity is a simple function of the net column cross-sectional area. Experimental results (Exper. *v*) show variation attributed to uncertainty in the effective porosity, which was found to vary ±20% from one packing to another.

Figure 3.5: Model Simulations of vertical velocity distribution for various PVP probe designs within a sealed column. A) shows the PVP (left) used for saturation tests and 2.46 cm PVP (right) with metal rod attached used in the PVP length comparison tests. Note that the 2.46 cm measurement is from the injection port to the upgradient end of the probe. B) is a model simulation of the probe used in iron-sand mixture and sand-only column saturation tests. C) demonstrates a model of the 4.75 cm PVP used in the column length comparison tests. D) models flow around a PVP representative of the probe implemented in the HRX Well. The bottom of the column is the upgradient constant head boundary, while the top of the column is the downgradient constant head boundary, inducing an overall flow from bottom to top. The blue area filling the space around the probes is a region of uniform seepage velocity, within a range of ±0.1 cm/d. The dark areas near probe edges and termini show the regions where the velocity rapidly approaches zero as flow encounters solid obstructions that force flow redirection.

Figure 3.6: PVP velocity versus estimated velocity (based on discharge measurements from the column assuming an average effective porosity of 0.3) for multiple lengths of PVP. The standard deviation of PVP velocity repeat tests is shown for each of the points. Shading indicates a potential ±20% uncertainty due to porosity differences between packings.

Figure 3.7: PVP velocity versus estimated velocity measured from column discharge (assuming a porosity of 0.33). "Saturated" represents the velocities based on a fully saturated column, "Air Injected" represents velocity measurements made for 7 days after injecting air through the PVP, and "Re-saturated" represents velocity measurements made within the re-saturated column. Arrows from the saturated column line to the re-saturated column line indicates the increase in measured PVP velocity after the column was re-saturated. Note that 7 days after air had been injected in the column, the velocity measurements returned to baseline. The curved arrow indicates the progression of days of measurements after injection of air. Point "1", one day after air was injected, displays the lowest PVP velocity. The points for the Saturated and Re-saturated

tests represent average values from 3-10 repeat tests for each point. The standard deviation of PVP velocity repeat tests is shown for each of the points. Gas generated by granular (zero valent) iron (ZVI) resulted in variable increases to the measured seepage velocity in a similarly prepared column.

Figure 3.8: Cutaway view of PVP inside HRX Well outlet cartridge. The cartridge for the inlet side of the well has the PVP orientation reversed to accommodate flow in the other direction.

Figure 3.9: Linear velocity measured by PVPs within the HRX Well and site gradient for specific sampling dates. Boxplots indicate the measured velocities for each sampling date. The average velocity for December 2018 (12/18) is the average of 8 measurements taken at both the inlet and outlet PVP. Since the inlet PVP was no longer functional after installation of the seals, the 4 measurements taken in April 2019 (4/19), 3 measurements in July 2019 (7/19), and 5 measurements in February 2020 (2/20) represent averages from the outlet PVP only. The dashed line indicates the gradient at the site measured during the same week PVP tests were conducted.

Figure 3.10: A) Visual representation of the effect of the HRX Well on the potentiometric surface during passive operation. B) Streamlines showing the extent of the capture zone for the HRX Well under conditions representative of those at the Vandenberg Air Force Base. The capture zone width of 25 m is comparable with the 15 m width calculated by Divine et al. (2018). The difference is attributed to the grid refinement. C) The 2D model indicated that the hydraulic gradient near and inside the HRX Well was, for practical purposes, linearly related to the regional gradient. This was also the case for the flow rate inside the well.

List of Tables

1.0 Introduction

This study was undertaken as part of a larger program sponsored by the Environmental Security Technology Certification Program (ESTCP), which is the Department of Defense's (DoD) environmental technology demonstration and validation program. The overall project was aimed at demonstrating, at the field scale, the HRX Well® for groundwater treatment. This thesis provides a scientific basis for the design and assessment monitoring of HRX Wells, but also contributes to the broader scientific literature concerned with the hydrologic characterization of granular porous media, both at the laboratory and field scales.

1.1 The HRX Well

Contamination of groundwater, the largest global source of drinking water, is common worldwide, by both natural or anthropogenic causes (Jeong, 2001; Moran et al., 2007; Thomas et al., 2009; Zhao et al., 2019; Bindal and Singh, 2019). To abate this problem, *in situ* treatment methods were developed to take advantage of cost and safety benefits that come with treating the contamination in place. Permeable reactive barriers (PRBs) (EPA source, 2003) were proposed to treat groundwater passively with minimal interference for land uses on the surface. However, PRBs can be expensive to install so the cost advantages are not experienced for several years after operations begin. The HRX Well® is a recent groundwater remediation technology that offers advantages similar to those of the PRB, but has design modifications that improve on the efficiency, cost, and ecological footprint of PRBs (Divine et al., 2018a; Divine et al., 2018b).

The HRX Well uses a horizontally-drilled well packed with highly permeable reactive treatment media. In low hydraulic conductivity (K) aquifers, the K contrast between the well and aquifer leads, without pumping, to an expansive capture zone that feeds contaminated water into the HRX Well. As the groundwater travels into the HRX Well, the contaminant(s) is either

removed or degraded by the treatment media. Finally, treated groundwater is released at the downgradient end of the well back into the aquifer (Figure 1.1). Divine et al. (2018b) implemented a pilot-scale project for the HRX Well technology in order to validate the field-scale design.

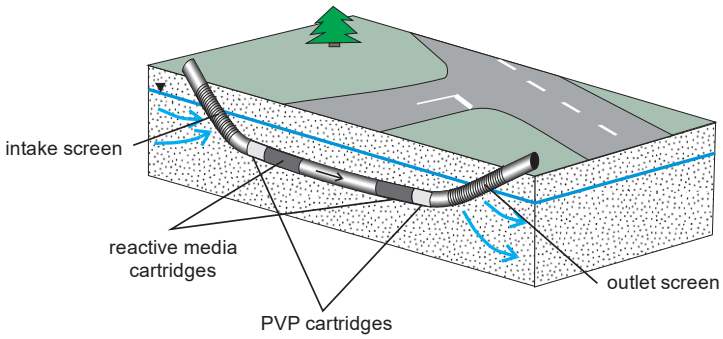

Figure 1.1: Schematic of the HRX Well treatment system. Blue arrows denote groundwater flow into and out of the well.

The HRX Well relies on a large *K* contrast between the packed media inside, and the aquifer material outside. However, simply packing the well with the coarsest material available (e.g., gravel) is not recommended because the matrix must blend uniformly with the reactive material and remain blended during the packing procedure. Therefore, a reliable laboratory assessment of the matrix material for use in the reactive media, and the *K* of the reactive media, are highly desirable for HRX Well design calculations. Grain size analysis is an important part of this process, since the choice of media with similar grain size distributions are less affected by size segregation during HRX Well packing than dissimilar media would be (Hogg, 2009). Grain size analysis has also been used to estimate *K,* although these methods are known for producing highly variable estimates of *K* where natural sediments and aquifer media are concerned (Devlin, 2015).

Permeametry is another laboratory-scale method for estimating *K* and may be considered superior to grain size analysis because the tests inherently include the dynamic nature of flow in the *K* estimations. However, once again, the representativeness of these tests has been found to be weak in many cases (e.g. Gierzcak *et al.*, 2005). Despite this somewhat discouraging prognosis for the usefulness of grain size analysis and permeametry in the current work, these methods have a surprisingly limited record concerning their application to *engineered porous media*. Addressing this gap in the literature is one of the goals of this thesis.

The performance of the HRX Well depends strongly on the capture of groundwater by the well, and this must be quantitatively predictable and verifiable for the purposes of well design and performance assessment. Divine *et al.* (2018b) described computational methods to fulfill the requirement for predictability. This leaves performance assessment as a major challenge yet to be formally demonstrated. Fully mapping a capture zone with monitoring wells is a possible approach but is unlikely to be practical in most cases. Augmenting a partially mapped capture zone with measurements of flow *inside* the HRX Well, however, could provide sufficient quantitative evidence of the well performance to satisfy performance assessment requirements. In order to monitor that internal flow rate, modified Point Velocity Probes (PVPs) (Labaky et al., 2007; Devlin et al., 2012; Labaky et al. 2009; Kempf et al., 2013) were designed with the aid of numerical modeling and laboratory testing, and applied to a field-scale HRX Well to evaluate the well performance.

1.2 Measuring Media Hydraulic Conductivity

An HRX Well is, in principle, able to treat a wide variety of groundwater contaminants because the treatment media it contains can be tailored to the target contaminants at the site undergoing treatment. Common methods for determining hydraulic conductivity include

laboratory scale testing by permeametry or grain size analysis, and field scale testing by slug tests, pumping tests, tracer tests, and model calibration (Fitts, 2013). In this work the emphasis was on preliminary laboratory scale testing of HRX Well media to inform design calculations. Field testing was reserved for aquifer characterization and HRX Well performance assessments at the end of the project. Specifically, grain size analysis and permeametry were both conducted with the hypothesis that the methods would be similarly accurate in estimating *K* for engineered porous media. This optimistic expectation was based on the observation that grain size analysis and permeametry, using reworked samples, would be similarly devoid of geologically imposed variations in the measured *K* values. The same would be true for engineered porous media.

1.2.1 Grain Size Analysis

Grain size analysis is a common method of estimating the hydraulic conductivity of granular porous media (Masch and Denny, 1966). The hydraulic conductivity of the media is often assumed to be largely influenced by the percent of finer grains in the sample. For example, many of the algorithms used in grain size analyses set d_{10} as the effective grain size in the calculations. The notation, d_{10}, represents the grain diameter for which ten percent (by weight) of the sample grains are smaller. Over twenty different methods of grain size analysis have been developed. These algorithms can be broadly separated into two categories: those based on the theory of flow through pipes and those arising empirically from relationships between grain size distribution and hydraulic conductivity (Rosas et al., 2014). In general, the empirical relationships are generated from limited data sets involving relatively homogeneous media (Shepherd, 1989; Hazen, 1893; Slichter, 1899). For this reason, in part, many studies have found them to lack accuracy when applied to heterogeneous field samples (Gierczak et al., 2006; Gallardo and Marui, 2007; Vienken and Dietrich, 2011; Rosas et al., 2014).

Efforts have been made to increase the diversity of data sets used in order to modify the equations and expand their scope. Categorizing samples by their depositional settings has also been suggested as a means of improving *K* estimation from grain size analysis (Shepherd, 1989; Rosas et al., 2014, 2015). However, hydraulic conductivity depends on a variety of factors that are unlikely to be captured by grain size analysis, including temperature, subtleties and variations in grain packing, cohesion, alignment (often associated with anisotropy in *K*), effective porosity and fluid pressure (Devlin, 2015; Schriever, 1930). Many of these issues are removed in the consideration of engineered homogenous media, so grain size may be better suited for characterizing this class of porous medium (Aubertin *et al*., 1996; Mondal, 2004; Scannell, 2016; Henderson, 2010; Côté *et al*., 2011; Choo *et al*., 2018).

1.2.2 Permeametry

Permeameters have been developed for laboratory and field applications (Klute and Dirksen, 1986; Chen, 2004; Chappell and Lancaster, 2007). The hydraulic conductivity of a sample is measured by inducing a hydraulic gradient across a contained sample of the porous medium and measuring either steady state outflow (constant head permeameter) or changes in hydraulic head (falling head permeameter) over time. In some cases, permeametry may be conducted on samples collected in core in order to preserve the porous medium structure and achieve more accurate estimates of *K*. For media with very low hydraulic conductivities, such as silty or clay-containing samples, the falling-head test is recommended. For highly permeable media, such as sand, a constant-head test is recommended (Klute and Dirksen, 1986).

One highly studied source of error in permeametry is the sample size, which must be small (compared to field applications requiring *K* estimates) to accommodate the permeameter apparatus. Small samples may not adequately represent scale-dependent factors that affect

hydraulic conductivity in heterogeneous media, particularly at the field scale. These factors may include preferential flow through macropores and packing variations between interconnected strata or sediment lenses (Schultze-Makuch et al., 1999; Davis et al., 1999; Lai and Ren, 2007; Zhang, 2019). For example, Schultze-Makuch et al. (1999) compared *K* from permeametry to estimates from slug tests, pumping tests, and regional flow models and showed an increase in the *K* estimates as the measurement scale increased; permeametry produced the lowest *K* estimates and represented the smallest sample size. In the case of engineered porous media, highly homogenous media can be packed in a controlled fashion so scale dependencies can reasonably be expected to be small (or absent).

A challenge for permeametry where highly permeable media are concerned is to account for frictional losses caused by the permeameter itself. Such losses may be caused by small outlets, friction in pipes, head losses in right-angle connectors or screens – i.e. any part of the system where flow might be restricted (Kandra et al., 2014; Nijp et al, 2017; Prodanovic et al., 2018). Nijp et al. (2017) found a dependency of measured hydraulic conductivity on the hydraulic head applied in the permeameter and attributed this to turbulence and non-Darcian flow within the highly permeable sediments under study. Klute and Dirksen (1986) recommended that tests involving the fractions coarser than medium sand be limited to hydraulic gradients less than between 0.5 and 1. The friction in a permeameter can be partially estimated using equations, such as the Darcy-Weisbach and Hazen-Williams equations, as a further check on how much the hydraulic conductivity measurements might be influenced by hydraulic head loss in the permeameter (Hazen and Williams, 1914; Simmons, 2008).

1.3 Monitoring Instrumentation: Point Velocity Probes

Point Velocity Probes (PVPs) have been utilized in numerous applications, due to the high importance of knowing the speed and direction of groundwater flow in all facets of hydrogeology. The original PVP was designed for application in aquifers using dedicated boreholes that collapsed against the instrument (Labaky et al., 2007). Recent modifications have resulted in PVPs suitable for applications in stream- and lakebeds (SBPVP) (Cremeans and Devlin, 2017), in addition to wells and open boreholes (IWPVP) (Osorno and Devlin, 2018).

To date, none of the PVP modifications have measured flow along an extended length of the long axis of the probe (Figure 1.2). For example, the original PVP measures flow around about 2 to 6 cm of the probe surface (depending on the probe orientation to the flow direction) (Labaky et al., 2007)(Figure 1.2A). The SBPVP has an operational surface distance of no more than about 2 cm (Cremeans and Devlin, 2017)(Figure 1.2B). The IWPVP directs water through an open probe volume that does not require the tracer to contact the probe surface – though the channels containing the detectors are sufficiently narrow (4.5 mm) that some minor drag on flow might occur (Osorno and Devlin, 2018)(Figure 1.2C). The adaptation of a PVP for use inside an HRX Well – actually, inside a cylindrical cartridge that was inserted into the HRX Well – required the probe to be part of an assembly of extended length with flow contacting the assembly over its entirety. This assembly was oriented parallel to the long axis of the HRX Well, and in the final design consisted of a central stainless steel support rod about a meter in length, and a plastic PVP body at least 10 cm long (Figure 1.2D). Before adopting this design, three considerations had to be addressed experimentally. First, a maximum distance between the end of the assembly and the tracer release/detection zone, that still avoided flow anomalies at the terminal edges of the assembly from biasing velocity measurements, had to be determined.

Second, it was necessary to demonstrate that the long contact distance along the assembly leading up to the detectors did not bias velocity measurements due to friction on the probe surface.

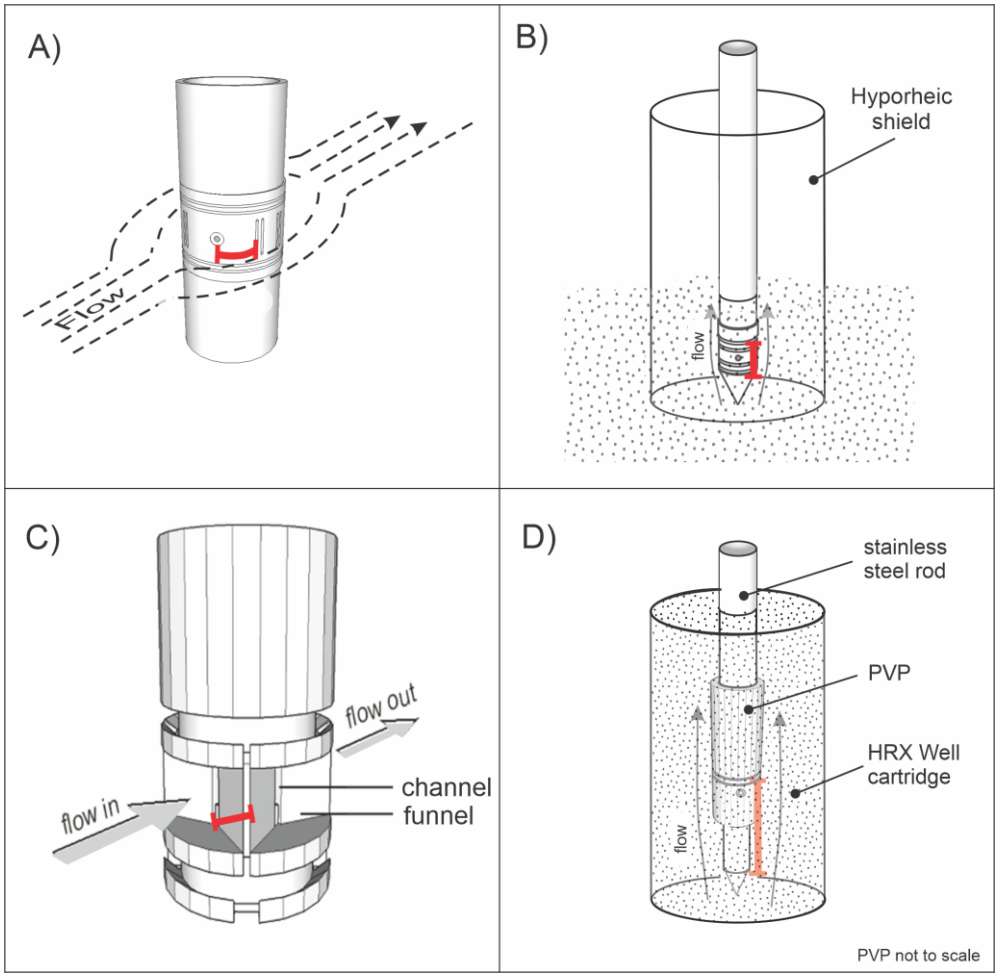

Figure 1.2: Schematics of 4 PVP designs. Red lines show the path length of flow that might affect tracer migration and velocity measurement accuracy. A) The original PVP used in direct contact with the aquifer material has minimal water flow contact with the surface along the cylinder for the path of the tracer from the injection port to the detectors. B) The SBPVP, measuring vertical flow through a streambed or lakebed, has minimal point of contact for flow along the surface before reaching the measurement point. C) The IWPVP, for well and borehole use, has flow through an open chamber in the center with minimal contact through the probe. D) The PVP installed near the downgradient end of the HRX Well includes a relatively long surface of contact along a metal cylinder for the flow of water prior to reaching the location for velocity measurement.

Finally, a PVP placed in a cartridge occupies some of the cross-sectional area of the cartridge. It was necessary to establish that the PVP did not obstruct the flow in the HRX Well severely enough to be of practical importance.

In addition to the hydraulic issues linked to PVP design, discussed above, the use of a PVP in a reactive medium raises the possibility that the medium itself might change over time, with an effect on flow, such as might occur by gas production or the accumulation of solid reaction products (e.g. through corrosion reactions). This issue was of particular concern to the HRX Well technology because the field test (see section 1.3 Field Site, below) involved a reactive medium containing 35wt.% granular iron mixed with coarse sand in order to degrade trichloroethene and other chlorinated compounds. Granular iron is known to react with water, producing hydrogen gas and hydroxyl ions. The latter can combine with iron to precipitate iron hydroxides and oxyhydroxides (Reardon, 1995; Zhang and Gillham, 2005). Of these two side-reactions, porosity loss due to gas production is most likely to exert a short term effect on the *K* of the medium, as demonstrated in treatability testing completed during the granular iron selection process of the greater HRX Well project (Divine *et al,* 2017). In this study, preliminary testing was undertaken to assess the ability of the PVP technology to respond to porosity loss due to gas production (supplementary note: after the desaturated media experimentation was begun, the project managers decided to deploy the PVPs in sand-only cartridges where gas production was not going to occur. Nonetheless, the experiments were completed for the benefit of future work that might benefit from the resulting insights).

1.4 Field Site

The field component of the work in this study was conducted at the Vandenburg Air Force Base in California. The target contaminants for treatment by the HRX Well were trichloroethylene (TCE), and its dechlorinated daughter products, dichloroethene (DCE) and vinyl chloride (VC). These are common contaminants worldwide that have been linked to symptoms such as central nervous system depression, immunotoxicity, nephrotoxicity, congenital and developmental defects, and carcinogenic effects (Chiu et al., 2013). Compared to the EPA Maximum Contaminant Level (MCL) standards of 5 μg/L of TCE, 7 μg/L for DCE (all isomers) and 2 μg/L for VC in drinking water, the study site at Vandenberg was found to have on the order of 50,000 μg/L of TCE in the groundwater in some areas (EPA, 2018; Divine et al., 2018b). Since TCE is degradable with granular iron (Gillham and O'Hannesin, 1994; Divine, 2018b), the HRX Well reactive medium was prepared with this material and mixed with sand. The purpose of the sand was to limit porosity loss over time by minimizing gas production rates (less iron per cubic meter leads to less reaction with water and less hydrogen production) and ensuring open porosity was maintained as iron corrosion products accumulated over the longer term (Mackenzie et al., 1999).

1.5 Statement of Objectives

The primary objective of this project was to assist with the design and assessment of the hydraulic performance of the a pilot HRX Well for passive groundwater treatment. In the process, an additional objective was to contribute to the greater scientific knowledge base concerned with porous media characterization 1) at the laboratory scale, for application at the field scale, 2) by direct velocity measurements in saturated and unsaturated media and 3) the adaptation of simple two dimensional models to the problem of horizontal well hydraulics and

PVP testing in a confined cylindrical space. These greater objectives can be subdivided into the following specific goals:

1. Assessment of HRX Well hydraulic performance
    a. Conduct grain size analysis and permeametry at a laboratory-scale in order to estimate the hydraulic conductivity (K) of the field-scale, engineered granular porous media to be packed into the HRX Well.
        i. Compare 16 grain size analysis algorithms to determine which show the most promise for accurately predicting K for a medium grain sand with d_{10} ~ 0.2 mm (initially selected for HRX Well packing material), and mixtures of this material with various fractions of granular iron (d_{10} ~ 0.3).
    b. Modify PVPs for deployment in cylindrical cartridge environments, in this case with field validation by application in HRX Wells.
    c. Measure PVP seepage velocities in the installed HRX Well at Vandenburg Air Force Base in California to assess remediation performance.
2. Broader scientific goals
    a. Addressing scale-dependency issues by demonstrating that bench-scale measurements can accurately reflect larger scale behavior. If this is observed, the work will provide evidence that scale alone does not determine the representativeness of measured K values. Rather, it follows that scale is only a proxy for the geologic depositional processes that determine porous media structure.

b. Measure *K* for different ratios of medium grain sand to coarse-grained granular iron in porous medium mixtures, using grain size analysis and permeametry. This work will help to assess the role of porous media mixtures on *K*.

c. Produce PVP laboratory sand columns with varying levels of saturation and compare this to PVP iron-sand mixture column tests to determine i) the sensitivity of PVP velocity measurements to saturation level and ii) to demonstrate the magnitude of the effect of gas production in granular iron (and by extension in any gas-producing porous medium, including biologically active media) on seepage velocity.

d. Develop 2D flow models to accurately assess flow regimes within an HRX Well monitoring cartridge and overall HRX Well system. These models will be validated by comparison with actual physical systems. If successful, this effort could assist with future design work involving the HRX Well, or other horizonal well installations by justifying the use of small, simple models in these activities.

1.6 References

Aubertin, M., Bussiere, B., Chapuis, R. P. 1996. Hydraulic conductivity of homogenized tailings from hard rock mines. Canadian Geotechnical Journal, 33 (3):470-482. doi: https://doi.org/10.1139/t96-068

Baciocchi, R., Boni, M. R., D'April, L. 2003. Characterization and Performance of Granular Iron as Reactive Media for TCE degradation by Permeable Reactive Barriers. *Water, Air, and Soil Pollution*, 149 (1-4): 211-226. doi: https://doi.org/10.1023/A:1025675805073

Bindal, S., Singh, C. K. 2019. Predicting groundwater arsenic contamination: Regions at risk in

highest populated state of India. *Water Research*, 159: 65-76. doi: https://doi.org/10.1016/j.watres.2019.04.054

Chen, X. 2004. Streambed hydraulic conductivity for rivers in south-central Nebraska. *Journal of the American Water Resources Association*, 40 (3): 561-574. doi: https://doi.org/10.1111/j.1752-1688.2004.tb04443.x

Chiu, W. A., Jinot, J., Scott, C. S., Makris, S. L., Cooper, G. S., Dzubow, R. C., Bale, A. S., Evans, M. V., Guyton, K. Z., Keshava, N., Lipscomb, J. C., Barone, S., Fox, J. F., Gwinn, M. R., Schaum, J., Caldwell, J. C. 2013. Human health effects of trichloroethylene: key findings and scientific issues. *Environmental Health Perspectives*, 121(3): 303-11. doi: 10.1289/ehp.1205879

Choo, H., Lee, W., Lee, C., Burns, S. E. 2018. Estimating Porosity and Particle Size for Hydraulic Conductivity of Binary Mixed Soils Containing Two Different-Sized Silica Particles. Journal of Geotechnical and Geoenvironmental Engineering, 144 (1): 04017104. doi: https://doi.org/10.1061/(ASCE)GT.1943-5606.0001802

Côté, J., Fillion, M-H., Konrad, J-M. 2011. Estimating Hydraulic and Thermal Conductivities of Crushed Granite Using Porosity and Equivalent Particle Size. Journal of Geotechnical and Geoenvironmental Engineering, 137 (9): 834-842. doi: https://doi.org/10.1061/(ASCE)GT.1943-5606.0000503

Devlin, J. F. 2015. HydrogeoSieveXL : an Excel-based tool to estimate hydraulic conductivity from grain size analysis. *Hydrogeology Journal*, 23 (4), 837-844. doi: https://doi.org/10.1007/s10040-015-1255-0

Devlin, J. F., Schillig, P. C., Bowen, L., Critchley, C. E., Rudolph, D. L, Thomson, N. R.,

Tsoflias, G. P., Roberts, J. A. 2012. Applications and Implications of Direct Groundwater Velocity Measurement at the Centimeter Scale. *Journal of Contaminant Hydrology,* 127 (1-4): 3-14. doi: https://doi.org/10.1016/j.jconhyd.2011.06.007

Divine, C., Crimi, M., Devlin, J.F. 2017. Treatability test study report, demonstration and validation of the Horizontal Reactive Media Treatment Well (HRX Well®) for managing contaminant plumes in complex geologic environments. ESTCP Project 16 EB-ER1-046, 56 pp.

Divine, C. E., Roth, T., Crimi, M., DiMarco, A. C., Spurlin, M., Gillow, J., Leone, G. 2018a. The Horizontal Reactive Media Treatment Well (HRX Well®) for Passive In-Situ Remediation. *Groundwater Monitoring and Remediation*, 38 (1): 56-65. doi: https://doi.org/10.1111/gwmr.12252

Divine, C. E., Wright, J., Wang, J., McDonough, J., Kladias, M., Crimi, M., Nzeribe, B. N., Devlin, J. F., Lubrecht, M., Ombalski, D., Hodge, B., Voscott, H., Gerber, K. 2018b. The horizontal reactive media treatment well (HRX Well®) for passive in situ remediation: Design, implementation, and sustainability considerations. *Remediation*, 28 (4): 5-16. doi: https://doi.org/10.1002/rem.21571

EPA. 2003. NATO/CCMS Pilot Study: Evaluation Of Demonstrated And Emerging Technologies For The Treatment And Clean Up Of Contaminated Land And Groundwater (Phase III) 2002 Annual Report. *NSCE*.

EPA. "National Primary Drinking Water Regulations." 22 Mar. 2018, Retrieved from https://www.epa.gov/ground-water-and-drinking-water/national-primary-drinking-water-regulations

Firdous, R., Devlin, J. F. 2018. Surface carbon influences on the reductive transformation of

TCE in the presence of granular iron. *Journal of Hazardous Materials*, 347: 31-38. doi: https://doi.org/10.1016/j.jhazmat.2017.12.043

Fitts, C. R. *Groundwater Science*, 2nd ed., Academic Press, Waltham, MA, 2013.

Gierczak, R. F. D., Devlin, J. F., Rudolph, D. L. 2006. Combined use of field and laboratory testing to predict preferred flow paths in an heterogeneous aquifer. *Journal of Contaminant Hydrology*, 82(1-2): 75-98. doi: https://doi.org/10.1016/j.jconhyd.2005.09.002

Gu, B., Phelps, T. J., Liang, L., Dickey, M. J., Roh, Y., Kinsall, B. L., Palumbo, A. V., Jacobs, G. K. 1999. Biogeochemical Dynamics in Zero-Valent Iron Columns: Implications for Permeable Reactive Barriers. *Environmental Science and Technology*, 33 (13): 2170-2177. doi: https://doi.org/10.1021/es981077e

Henderson, A. D. 2010. Solids formation and permeability reduction in zero -valent iron and iron sulfide media for permeable reactive barriers. ProQuest Dissertations Publishing. Web.

Hogg, R. 2009. Mixing and segregation in powders: evaluation, mechanisms and processes. *KONA Powder and Particle Journal*, 27: 3-17. doi: https://doi.org/10.14356/kona.2009005

Jeong, C. H. 2001. Effect of land use and urbanization on hydrochemistry and contamination of groundwater from Taejon area, Korea. *Journal of Hydrology*, 253 (1-4): 194-210. doi: https://doi.org/10.1016/S0022-1694(01)00481-4

Kempf, A., Divine, C.E., Leone, G., Holland, S., Mikac, J. 2013. Field performance of point velocity probes at a tidally influenced site. *Remediation*, Winter. doi: 10.1002/rem, 37-61.

Labaky, W., Devlin, J. F., Gillham, R. W. 2007. Probe for Measuring Groundwater Velocity

at the Centimeter Scale. *Environmental Science & Technology,* 41 (24): 8453-8458. doi: 10.1021/es0716047

Labaky, W., Devlin, J.F., Gillham, R.W. 2009. Field comparison of the point velocity probe with other groundwater velocity measurement methods. *Water Resources Research*, 45 (4). doi: 10.1029/2008WR007066.

Mackenzie, P. D., Horney, D. P., Sivavec, T. M. 1999. Mineral precipitation and porosity losses in granular iron columns. *Journal of Hazardous Materials*, 68 (1-2): 1-17. doi: https://doi.org/10.1016/S0304-3894(99)00029-1

Moran, M. J., Zogorski, J. S., Squillace, P. J. 2007. Chlorinated Solvents in Groundwater of the United States. *Environmental Science and Technology*, 41 (1): 74-81. doi: https://doi.org/10.1021/es061553y

Mondal, P. K. 2004. Performance evaluation of fabric aided slow sand filter. University of Windsor (Canada), ProQuest Dissertations Publishing. MQ96402.

Orth, S., Gillham, R. W. 1995. Dechlorination of Trichloroethene in Aqueous Solution Using Fe^0. 1995. *Environmental Science and Technology*, 30 (1): 66-71. doi: https://doi.org/10.1021/es950053u

Scannell, L. W. 2016. An analysis of performance criteria of porous ceramic water filter production methods. State University of New York at Buffalo, ProQuest Dissertations Publishing. 10163904.

Senzaki, T., Kumagai, Y. 1989. Removal of chlorinated organic compounds from wastewater by reduction process: II. Treatment of trichloroethylene with iron powder. *Kogyo Yosui*, 369: 19-25 (in Japanese).

Simmons, C. T. 2008. Henry Darcy (1803–1858): Immortalised by his scientific legacy.

Hydrogeology Journal, 16 (6): 1023-1038. doi: 10.1007/s10040-008-0304-3

Thomas, M. A., Engel, B. A., and Chaubey, I. 2009. Water Quality Impacts of Corn Production to Meet Biofuel Demands. *Journal of Environmental Engineering,* 135 (11):1123–1135. doi: 10.1061/(ASCE)EE.1943-7870.0000095.

Williams, G. S., Hazen, A. *Hydraulic Tables: The Elements of Gagings and the Friction of Water Flowing in Pipes, Aqueducts, Sewers, Etc. as Determined by the Hazen and Williams Formula and the Flow of Water Over Sharp-edged and Irregular Weirs, and the Quantity Discharged, as Determined by Bazin's Formula and Experimental Investigations Upon Large Models*. 2nd Ed., New York, John Wiley and Sons, 1914.

Zhang, Y., Gillham, R.W. 2005. Effects of gas generation and precipitates on performance of Fe0 PRBs. *Ground Water*, 43 (1): 113-121. doi: https://doi.org/10.1111/j.1745-6584.2005.tb02290.x

Zhao, Y., Lin, L., Hong, M. 2019. Nitrobenzene contamination of groundwater in a petrochemical industry site. *Frontiers of Environmental and Science Engineering*, 13: 29. doi: https://doi.org/10.1007/s11783-019-1107-6

2.0 Grain Size Analysis and Permeametry for Estimating Hydraulic Conductivity In Engineered Porous Media

2.1 Abstract

Grain size analysis and permeametry are common methods for estimating the hydraulic conductivity (*K*) of porous media. It is well known that these methods have limited accuracy when they are used to characterize natural sediments. However, hydrogeological research has increasingly introduced technologies dependent on engineered porous media that may be less problematic because complex geologic structures are eliminated in the lab and field-scale packings. The recently introduced Horizontal Reactive Media Treatment Wells (HRX® Wells), for in situ, passive remediation of groundwater is one such example. The HRX Well passively collects groundwater and directs it through a horizontal pipe packed with an engineered porous medium. In this project, grain size analysis was conducted for sand and sand-iron mixtures to estimate *K* using the 16 algorithms provided in the HydrogeoSieveXL2.3.2 software. The results were compared to *K* determined by permeametry and a field-scale column, 30 cm long and 25 cm in diameter, representing an HRX Well. The best comparability of *K* estimates from grain size analysis and permeametry were obtained using the USBR, Slichter, and Shepherd *K* estimation methods. These also showed good agreement between lab-scale and field-scale *K* estimations, with reproducibility within the range ±20%. This study shows that laboratory *K* estimations can be representative across various relevant scales, including the field-scale, for engineered porous media. This finding extends to filter packs, and other engineered porous media design methods by emphasizing and demonstrating one case of accuracy in lab-scale permeability estimation for field-scale implementations.

2.2 Introduction

As contaminant hydrogeologists have advanced our understanding and appreciation of flow and reactive processes in aquifers, in situ remediation approaches have become varied and increasingly common. In support of this evolution, the application of engineered porous media to passively control flow or foster contaminant transformations has emerged, for example, permeable reactive barriers. To support such field activities, accurate and pragmatic methods to determine and optimize the hydraulic conductivity (K) of engineered porous media, in the laboratory, would be of great advantage. Surprisingly, there are few studies that demonstrate this kind of corroborative link. The design of well filter packs involves laboratory testing of porous media for field use, but the emphasis is on filtering the fine fraction of the aquifer sediments; an accurate determination of hydraulic conductivity is not required, as long as there is reasonable confidence that the K of the filter pack is greater than that of the aquifer.

A small number of investigations have made preliminary progress in estimating K for purely granular media to support field deployments, engineered for flow control. Devlin and Barker (1999) performed a field experiment involving a nutrient injection wall comprising an engineered sand installed in a fine sand aquifer. The objective was to establish a high permeability contrast between the wall and the aquifer to facilitate the flushing of the wall during periodic nutrient injection phases. The engineered wall was designed on the basis of laboratory grain size analysis and performed in the field as required, suggesting the laboratory testing was reasonably representative of the later field performance. However, a detailed comparison of the field and laboratory hydraulic properties of the sand was not undertaken.

Another example is given by Bowles *et al.* (2000) who reported on the performance of a 'trench-and-gate' system consisting of interconnecting permeable trenches that served as

collectors of hydrocarbon-contaminated groundwater. The groundwater was directed by the trenches to a centralized "gate" where in situ treatment took place. To maximize the collection capacity of the trenches, they were backfilled with screened gravel. The permeability of the trenches was later evaluated by a pumping test. In this case, the engineered porous medium was only needed to establish a high permeability contrast with the aquifer, and detailed laboratory characterization was unnecessary.

Examples of studies involving laboratory tests *for designing* field-scale reactive treatment systems, have been reported (Burbery *et al.,* 2014; Domga *et al.*, 2015; Page, 2016). However, many of these are confounded by the transient nature of the medium and biproducts of its reactivity, such as precipitates or gas formation. It is common for such studies to focus on the elucidation of processes rather than on the corroborative measurement of K at both the laboratory scale and the field scale (e.g., Zhang and Gillham, 2005; Deo *et al*. 2010; Fronczyk and Pawluk, 2014; Liu and Fassman-Beck, 2016). Examples also exist of studies that limited the assessment of hydraulic performance to field measurements (Schipper *et al.*, 2004; van Driel *et al.,* 2006; Robertson *et al.,* 2007). The question "can laboratory-scale tests represent field-scale systems in engineered media?" cannot be easily addressed in these studies.

A recent example of a technology requiring engineered porous media is the Horizontal Reactive Media Treatment Well (HRX® Well). The HRX is a passive groundwater remediation technology that utilizes a horizontal well containing a highly permeable, reactive treatment medium (Divine *et al*., 2018a; Divine *et al*., 2018b). Establishing and maintaining a large contrast (factor of 100 or more) in K between the media within the well and the aquifer is required to achieve the design objective of maximizing the capture zone in the aquifer. However, simply defaulting to gravel as the primary fill material is not recommended since at

least three considerations must come into play: (1) the medium must be reactive and treat water to target levels within the residence time frame; (2) the medium must maintain high permeability over time; and (3) the medium must maintain a uniformly well-mixed blend of inert material (e.g. sand or gravel) and reactive solids, such as granular iron to prevent bi-passing of reactive material and assure an optimized *K*, which can be a function of grain size uniformity. Therefore, quick and inexpensive laboratory tests to determine and reliably predict the *K* of HRX Well packing media with a reasonably high level of accuracy would benefit the technology by improving the reliability of design calculations.

Two common laboratory methods for estimating hydraulic conductivity are grain-size analysis and permeametry. Grain size analysis is commonly preferred for reasons of convenience and cost. However, the indirect and empirical nature of the method has so far frustrated attempts to find a single algorithm that performs well for all porous media. As a result, many algorithms have been developed to address various sediment and soil types, and subsets of these have been compiled into convenient software packages over the years (Vuković and Soro, 1992; Kasenow, 2002; Aguilar, 2013; Devlin, 2015). Major sources of error for grain size analysis come from the accuracy of porosity values, the variability of grain shape and orientation that is represented by a shape factor in most algorithms (in field settings, the method of sediment deposition noticeably affects grain shape and orientation), loss of aquifer structure in sample handling, and variability in pore water pressures (Schriever, 1930; Barth *et al.*, 2001; Rosas *et al*., 2014; Devlin, 2015). Issues connected to the shape factor have been found to be least problematic for homogeneous media consisting of rounded grains in the size range of sand. Experience with angular grains in heterogeneous field samples indicates that errors in the

prediction of K over multiple orders of magnitude are common (Gierczak *et al*., 2006; Gallardo and Marui, 2007; Vienken and Dietrich, 2011).

Some engineering applications, in which the grain shape and packing can be highly controlled, have found grain size analyses to be of value (Aubertin *et al*., 1996; Mondal, 2004; Henderson, 2010; Côté *et al*., 2011; Scannell, 2016; Choo *et al*., 2018). However, most of these studies, including many in the geotechnical literature, only report grain size K estimates for the purposes of relative comparisons, or comparisons between laboratory methods, and the absolute accuracy of the K values *vis-à-vis* field scale is not evaluated in detail (St. Marseille, 1999; Rice, 2007; Michette *et al*., 2017).

Permeametry uses Darcy's Law to calculate K based on flow through a sample of granular material, under a controlled hydraulic gradient. The gradient may vary (falling head tests) or may be held constant (constant-head tests). The latter approach , which is in fact the method Henry Darcy used in his seminal work (Darcy, 1865), is preferred for coarse granular materials (Klute and Dirksen, 1986). Constant head permeametry is a well-established method with a lower measurement limit on K of about 0.14 m/d (Klute, 1965). Briefly, a porous medium sample is placed between two containment screens and saturated with water. A constant hydraulic head drop is maintained across the sample, and the flowrate is measured as the water passes through the sample (Freeze and Cherry, 1979). K (in units of L/T) can then be calculated from:

$$K = \frac{Q \times \ell}{A \times \Delta H} \tag{1}$$

where, ℓ is the sample height (L), A is the cross-sectional area of the permeameter (L^2), ΔH is the head drop along the permeameter (L), and Q is the flow rate (L^3/T). Here, generalized units are used with L = length and T = time, and we assume laminar flow with density and viscosity of the

fluid to be near that of fresh water at 20°C. This method has seen wide application in hydrogeology and engineering (Van den Berg and de Vries, 2003; Warith *et al*., 2004; Gierczak *et al*., 2006; Fassman-Beck *et al*., 2015). The accuracy of permeametry has been subject to numerous evaluations in studies where natural deposits were of concern. In these cases, it has often been reported that permeameter estimates of *K* are of limited quantitative value, due in part to the scale dependencies associated with *K,* and biases from sample handling (Schultze-Makuch *et al*., 1999; Gierczak *et al.,* 2006; Zhang *et al*., 2019).

In this work, it is hypothesized that the measurement of *K* for granular, engineered porous media by either grain size or permeameter techniques is representative of the field scale, because in the engineered media the mixing process is controlled and the engineered media in the field are therefore likely to retain similarities in packing compared to those in the laboratory tests, despite scale differences. This hypothesis is tested systematically for both permeametry and grain size analysis, and evaluated for a field-relevant scale using the HRX Well as an exemplar.

2.3 Methods

2.3.1 Grain size analyses

Grain size analysis was conducted on mixtures of a medium grain sand (provided by Arcadis as a potential HRX fill material) and 0% (100 g), 10% (560 g), 50% (604 g), and 100% granular iron by weight (200 g). The 0% and 100% samples were analyzed in duplicate. Size fractions were isolated using sieve screen sizes of 2, 1, 0.5, 0.355, 0.250, and 0.150 mm, shaken for 10 to 45 minutes, with the longer times reserved for the samples with the greater masses. Samples containing only iron were divided into size fractions using sieves of 4, 2, 1, 0.600, 0.250, and 0.125 mm. A subsequent decision to move from medium sand to a coarse sand for the HRX Well application prompted supplemental testing of samples involving the coarse-

grained sand. This material was analyzed using sieve sizes 2, 1, 0.850, 0.600, 0.500, and 0.355 mm. The HydrogeoSieveXL Excel® software (Devlin, 2015; v. 2.3.2 of the software available at http://www.people.ku.edu/~jfdevlin/Software.html, revised to include the Shepherd algorithm [Shepherd, 1989], was used to obtain estimates of *K* from the grain size curves). Porosity, which is a required input for most grain size analysis methods, was automatically calculated within the software for each individual grain size analysis using (Istomina, 1957; Vukovic and Soro, 1992; Devlin, 2015),

$$n = 0.255 * (1 + 0.83^{U}) \quad (2)$$

$$U = \frac{d_{60}}{d_{10}} \quad (3)$$

where *n* is total porosity, *U* is the uniformity coefficient, d_{10} is the grain size for which 10% of the sample size (in mass) is smaller, and d_{60} is the grain size for which 60% of the sample size is smaller. Effective porosity was estimated for the purposes of calculating seepage velocities. For sandy materials, these tend to be similar to, or slightly smaller than, values of total porosities (Equation 2) (Hudak, 1994). For the sandy media examined in this study, an effective porosity of 0.33 was adopted on the basis of previous work involving similar sediments (e.g., Morris and Johnson, 1967; Mackay *et al.,* 1986; Critchley *et al.*, 2014). It is acknowledged that the effective porosity is a source of some uncertainty, since some studies have reported lower values of the parameter in sandy sediments (e.g., 0.15 by Kempf *et al.*, 2013).

2.3.2 Permeametry

Permeameter tests were conducted using a Gilson HM-892 3-inch (7.6 cm) diameter permeameter with a glass column measuring 15 cm high. Tests were conducted with sample heights (ℓ) of approximately 7 cm (6.3 to 7.6 cm), corresponding to sand masses of about 500 g and samples containing iron not exceeding 700g. No samples contained grain sizes more than

0.4 cm in diameter (maximum iron grain size), and 95% of the grains in all media tested passed through the 0.2 cm sieve. According to the ASTM standard D2434 – 68 (ASTM, 1991), as reported by SERAS (2003), the 7.6 cm diameter permeameter is properly sized for all measurements reported here. The apparatus was configured for constant head operation (Freeze and Cherry, 1979) (Figure 2.1). For each medium (coarse sand, medium sand, and sand-iron mixtures), tests were performed in series marked by ever declining values of hydraulic gradient, *i*, until a value of hydraulic conductivity was obtained that was independent of *i*, that is, until the estimated *K* values in two successive tests with declining *i* values did not appreciably change. This established a gradient that would not impose notable frictional losses in the permeameter apparatus other than those caused by the porous medium (Nijp *et al*., 2017). Once the optimum *i* was obtained for a given medium, it was held constant throughout the subsequent tests. Permeameter tests were conducted on 0, 10, 25, 35, 50, 75, 85, and 100wt.% of iron mixed with a medium grain sand. Repeat experiments were conducted for 10 and 85wt.% of iron for quality assurance and control purposes (QAQC). Supplemental permeameter tests were also conducted on 0 and 35wt.% of iron mixed with coarse grain sand.

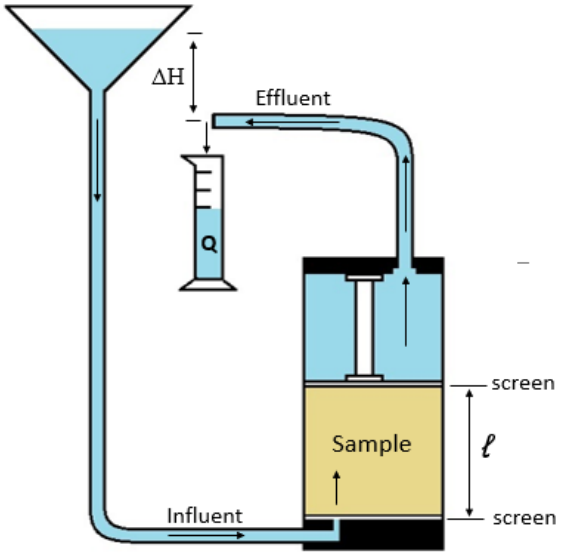

Figure 2.1: Schematic of the constant-head permeameter apparatus used in this study.

2.3.3 Column testing

Hydraulic conductivity was determined for the medium sand using a 25cm diameter (A = 491 cm^2), 30 cm high Plexiglas® column (Figure 2.6a) with ports suitable for connecting manometers at 2, 4, 6, 11, 16, and 21cm from the inlet. The manometers consisted of 0.3cm inside diameter tubes attached to sampling ports located 15cm apart (ℓ) (6 and 21cm from the inlet) on the column and secured on a vertical brace, as similarly seen in other work (Darcy, 1856; Freeze and Cherry, 1979; Devlin, 1994). The manometer tubes were clamped shut during normal column operation to minimize interference with flow in the column. For hydraulic gradient determinations, the clamps were opened and allowed at least 15min to equilibrate prior to measuring the water levels. The tubes were subsequently reclamped. The difference in water levels in the manometer tubes, ΔH, was measured with a caliper (± 0.02mm). The hydraulic gradient across the column was calculated ($i = \Delta H / \ell$), and K subsequently estimated using the Darcy equation (Equation 1).

Between manometer readings, flow in the column was monitored with a point velocity probe (PVP) designed to measure seepage velocity (v) in the direction of flow (Labaky *et al.*, 2007). The PVP tests were conducted with a tracer consisting of 1 g/L NaCl solution, injected in pulses of 0.3 mL per test, over a time interval between 12 and 25 seconds. A similar probe was built into a pilot test of the HRX Well, so comparisons of PVP-derived estimates of v with those calculated from Equation 4, using K values from grain size analyses and permeametry, were relevant to future field campaigns. Seepage velocities were calculated from

$$v = \frac{K}{n_e} \times \frac{\Delta H}{\ell} = \frac{Q}{A \times n_e} \tag{4}$$

where n_e is the effective porosity.

2.4 Results and Discussion

The duplicate pairs of grain size samples (100% sand and 100% iron) each yielded nearly identical grain size distributions indicating the sample sizes used were sufficiently large to be generally representative of the respective media. The grain size curves of unmixed samples of the medium sand and unmixed samples of granular iron both revealed low fractions of grains <0.2 mm (~ d_{10}), consistent with highly permeable media (Figure 2.2). The medium grain sand was found to be somewhat better sorted than the iron. In samples where these two media were mixed, the grain size distributions were nearly identical in the size range <0.4mm and exhibited slightly divergent curves in the higher size fractions (> 0.4 mm).

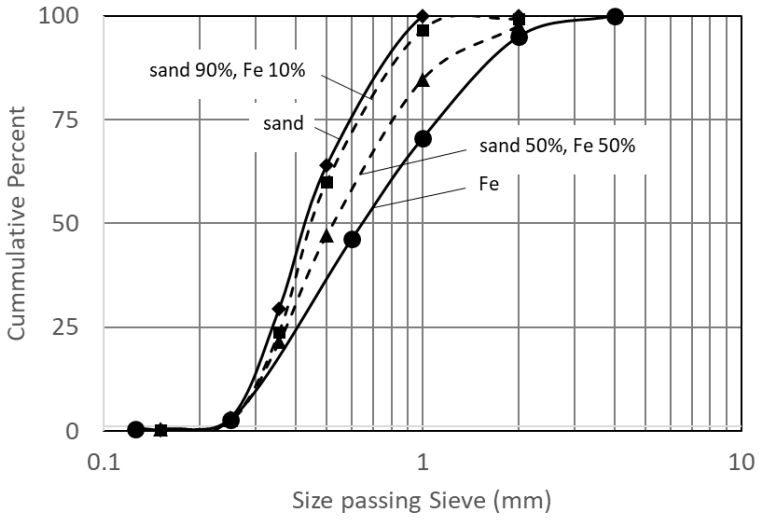

Figure 2.2: Grain size curves for medium grain sand and iron mixtures.

Despite the general similarities in the sand and iron grain size curves, the various grain size analysis algorithms in HydrogeoSieveXL produced *K* estimates that varied widely. The highest *K* value was generated with the Kozeny-Carman (K-C) algorithm (318 to 435 m/d, unmixed sand and iron, respectively), and the lowest *K* value came from the USBR algorithm (28 to 53 m/d) (Figure 2.3). As discussed in more depth below, most of the grain size analysis algorithms yielded *K* estimates larger than those obtained from permeametry. It has been suggested that such overestimates could be related to the handling of porosity in the various algorithms (Vienken and Dietrich, 2011). However, porosity as a source of disagreement between grain size-derived *K* and permeameter-derived *K* is unlikely to fully account for the order of magnitude differences (between permeametry and grain size analysis) observed here. A more likely explanation is that the variability between algorithms reflects the empirical nature of the functions and physical differences in the samples used to generate the relationships.

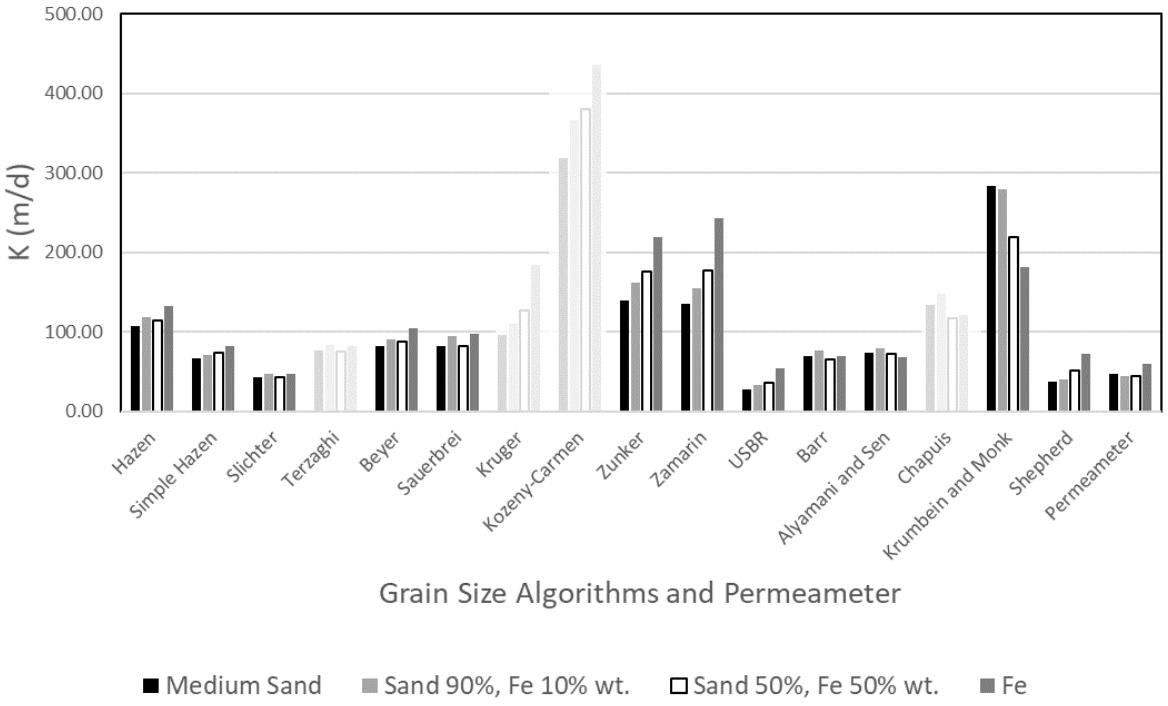

Figure 2.3: K values calculated from 16 grain size algorithms for medium grain sand and iron mixtures, compared with permeameter test results. The x-axis represents the different methods for determining K and the y-axis represents K values in m/d. Methods with faded bars represent algorithms with failed criteria for application to these grain size curves. 'Simple Hazen' refers to calculating K according to the following equation : $K = d_{10}^2$.

For the media considered in this work, three of the empirical grain size relationships available in HydrogeoSieveXL (Devlin, 2015) yielded *K* estimates that compared best with the results of the permeameter tests: Slichter, Shepherd, and USBR (Figures 2.4 and 2.5, Table 2.1). Details of all grain size analysis methods are found in Devlin (2015). The permeameter and Slichter methods produced *K* estimates that exhibited no clear trend across the sand-iron mixtures, up to 75% Fe. *K* increased in permeameter tests above this iron content, but the Slichter analysis did not capture this change. The USBR and Shepherd *K* estimates exhibited small, but steadily increasing, *K* with increasing iron content in the mixtures (Figure 2.5). No single grain size analysis method perfectly matched the trends observed in the permeameter test

results. For example, the Slichter and Shepherd methods best matched the permeameter results for samples dominated by the sand fractions, while the USBR method performed best when the iron fraction dominated.

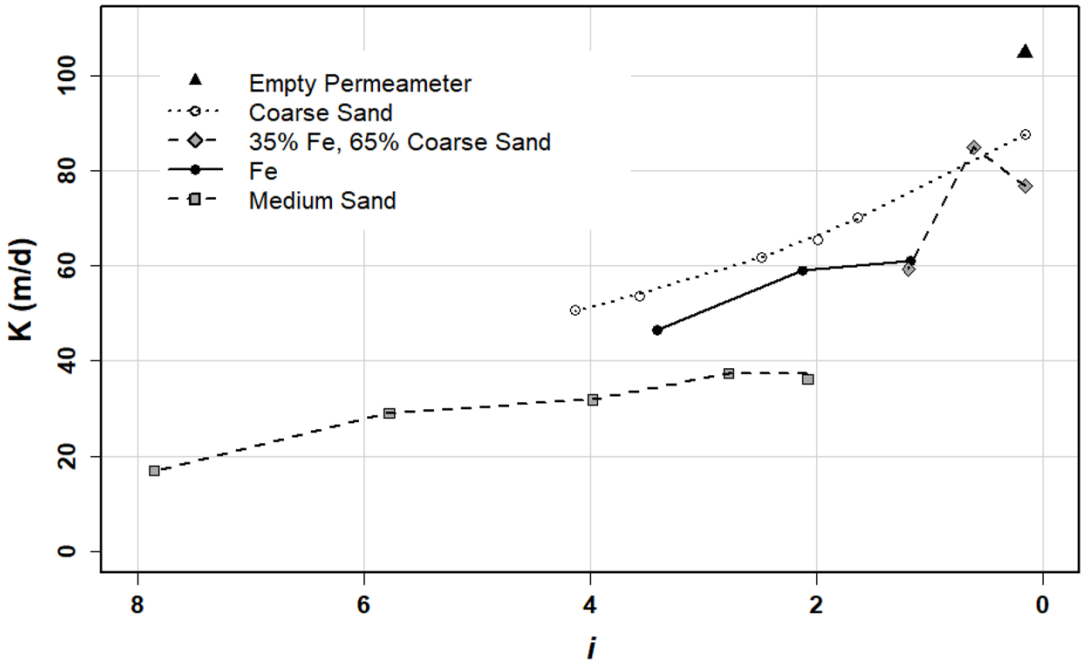

Figure 2.4: Graph showing effect of varying hydraulic gradient (i) on permeameter-measured hydraulic conductivities for medium sand, coarse sand, Connelly Iron, and the mix of 35% iron and 65% coarse sand. Also shown is the maximum measurable K, obtained from a permeameter containing no granular medium. Of the media tested, only the unmixed coarse sand did not show evidence of K independence from i at low i, suggesting the coarse sand had a K higher than the permeameter could measure.

Some corroboration of the preceding findings came from earlier work by Song *et al*. (2009), who examined the vertical hydraulic conductivity in streambeds composed of sand and gravel. Their samples exhibited grain size curves similar in character to those shown in Figure 2.2. They compared predictions from the algorithms of Hazen, Terzaghi, Beyer, Kozeny, Sauerbrei, Slichter, USBR, and Shepherd. As in the current study, they found that the USBR, Slichter, and Shepherd *K* values were closest to measured *K* values from permeameter tests. Moreover, the other methods overestimated *K,* with the Kozeny-Carman and Hazen methods yielding the

largest overestimates, also consistent with this work. Blohm (2016) conducted permeametry tests on two samples of artificially graded sand, again with grain size distributions similar to those found in this work and concluded that USBR gave the most accurate estimates, although the other algorithms they considered performed similarly.

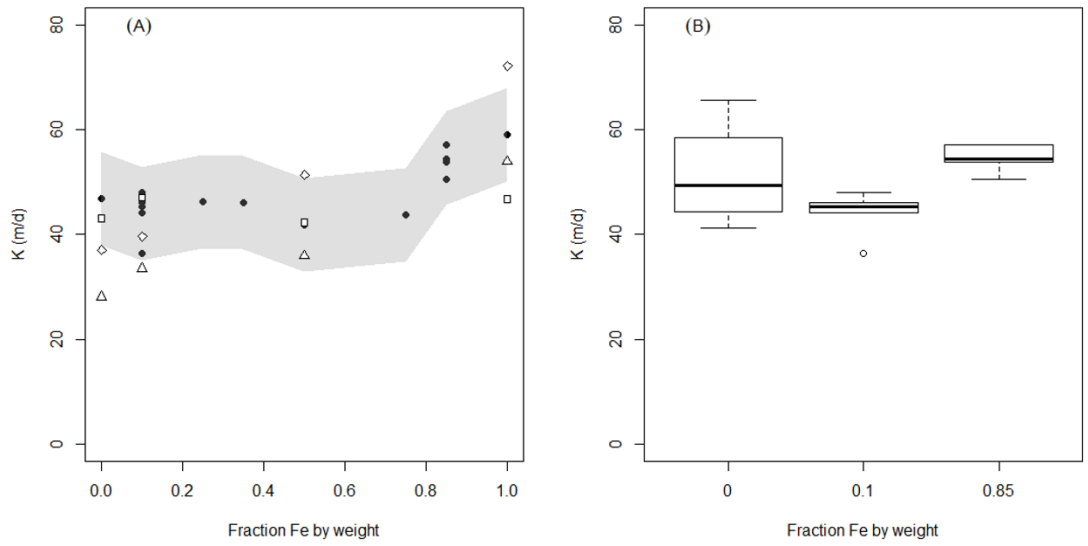

Figure 2.5: (A) K values for permeameter tests (•) on medium grain sand and iron mixtures. The shaded area represents the 95% confidence range of estimated K for each medium, based on the reproducibility of tests on the 90% sand/10% iron samples. Estimates of K are also shown for the Slichter (□), USBR (Δ), and Shepherd (◊) grain size algorithms. (B) Boxplots showing the spread in replicate tests for the sand-packed column (Fraction Fe = 0), and permeameter tests for two mixtures of sand and iron (10% Fe and 85% Fe).

Table 2.1: Summary of grain size analysis methods found to compare best to permeametry for the porous media considered.

Source	N	φ(*n*)	d_e	Applicable Conditions
USBR (United States Bureau of Reclamation) (Bialas, 1966)	*(4.8 × 10-4)(100³)*	*1.0*	$d_{20}^{1.15}$	*Medium grained sands with U < 5; derived for T = 15 °C*
Slichter (1898)	*1 × 10⁻²*	$n^{3.287}$	d_{10}	*0.01 cm < d_{10} < 0.5 cm*
Shepherd (1989)	*142.8, channel deposits[1]* *489.6, beach sand* *1632, dune sand*	*1.0*	$d_{50}^{(r/2)}$ *r= 1.65, channel deposits[1]* *r= 1.75, beach sand* *r=1.85, dune sand*	*0.0063<d_{50}<2*

The general form of the equation for K is: $K = \frac{\rho g}{\mu} N \varphi(n) d_e^{\,2}$ *Where, ρ is the temperature-dependent water density (g/mL), g is the gravitational constant (cm/s²), μ is the temperature-dependent dynamic viscosity of water (g/cm/s), N is a case-specific constant regarded as a 'shape factor', φ(n) is a function of porosity, and d_e is an effective grain size or function of the grain size distribution (equations adopted from Devlin, 2015).*

[1] *Used as default in this work.*

Reliable measurements of *K* for the medium sand and iron media required hydraulic gradients in the permeameter less than 3 and 1, respectively, to limit head losses to the packed medium rather than the apparatus (Figure 2.4). The upper limit on measurable *K* values with the equipment used here was determined to be 105 m/d, by conducting a test with an empty permeameter and a hydraulic gradient of about 0.1 to 0.2. Calculations performed with the Darcy-Weisbach equation and Hazen-Williams equation suggested that about 10% of the head drop in (empty) apparatus was attributable to inlet and outlet tubing. The remainder was presumably due to the ports and screens inside the permeameter. The maximum measurable value of *K* was greater than the estimates of *K* determined for either medium sand or iron in the permeameter tests, lending confidence to the validity of those permeameter tests. Note that tests

with the coarse sand sample did not appear to plateau with declining *i*, suggesting a *K* in excess of the 105 m/d limit of the permeameter (Figure 2.4).

The permeameter tests showed that the granular iron medium was characterized by a *K* about 30% higher than that of the medium sand. In mixtures of the two media, statistically indistinguishable *K* values, at the 95% confidence level, were obtained for the 0, 10, 25, 35, 50, and 75wt.% of iron-sand media (Figure 2.5a). The influence of the higher permeability iron medium on the mixtures only began to emerge with iron fractions of 0.85 (85wt.%) or greater. Above this quantity of iron, the *K* rose steadily to the value for the 100% iron medium. A *t*-test of the mean *K* values from 5 replicate tests for each of the 10% Fe and 85% Fe mixtures indicated a statistically significant difference with 95% confidence ($p = 0.003$).

As a final check on the representativeness of the *K* estimates from grain size analyses and permeametry, a medium sand was packed into a 30cm long, 25cm diameter, column with dimensions approaching those of a field-scale HRX Well (Figure 2.6a). A constant flow rate (3.3 to 7.5 mL/min in four individual tests) was maintained by pumping and the hydraulic head drop (0.035 to 0.05 cm) was measured across the column (Figure 2.6b). The *K* for the sand was estimated to be between 42 and 50 m/d, in good agreement with the range of estimates arising from the permeameter and preferred grain size tests (Slichter, USBR, Shepherd) (Figures 2.4 and 2.5).

A PVP installed in the column was used to measure the seepage velocity directly with the result that measured *v* values were in the range of (one standard deviation) 38 to 60 cm/d. Since the relevant parameter for any field application – in particular, the HRX Well system – is the velocity of the water (or flux), which controls residence times, *K* values determined in the laboratory tests were converted to corresponding v for comparison with PVP results.

Assuming an n_e of 0.33, which is commonly considered representative of sand media, the estimated values of K, and a column area of 483 cm^2 (obtained by subtracting the area of the probe from the total area in the column), the seepage velocity was predicted to be between 30 and 51 cm/d (Equation 5). The closeness of this agreement suggests the estimated K values are suitable for HRX Well design purposes with high expectations of matching field performances.

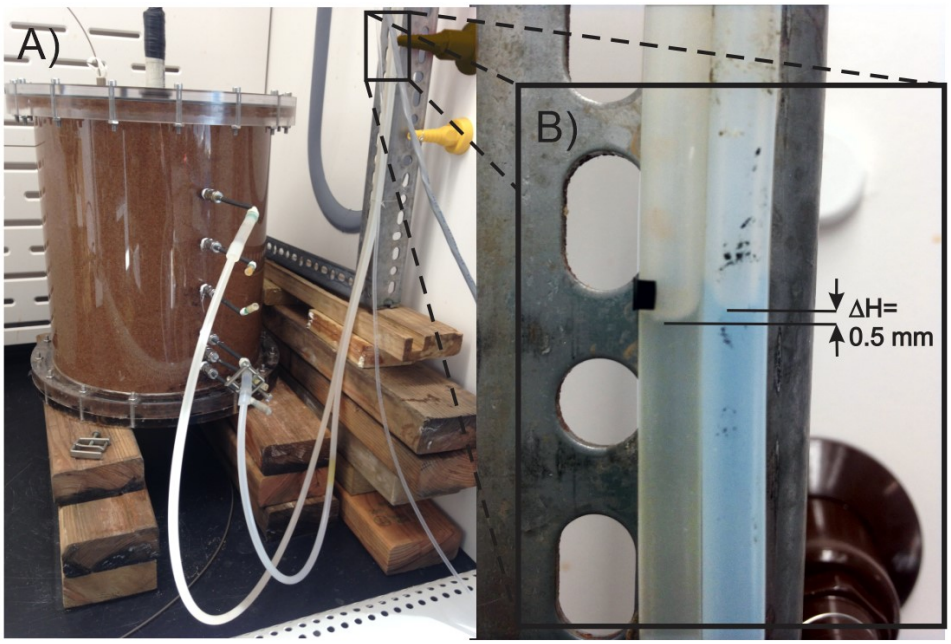

Figure 2.6: (A) Pressurized column with manometers attached to two ports located along the length of the column, 6 cm and 21 cm from the column inlet. (B) Tubing (shown close-up) was strapped vertically against a metal frame for easy water level measurement. ΔH = 0.5 mm indicates the difference in total hydraulic head between the two ports.

2.5 Conclusion

Sixteen grain size algorithms were employed to estimate K in reactive media consisting of granular iron and sand in various proportions. It is concluded here that three grain size analysis algorithms provided K estimates that compared well with estimates of K from permeametry and a field-scale mock HRX Well column (sand-only case). The preferred grain size analysis methods were the USBR, Slichter, and Shepherd methods.

It is further concluded that engineered reactive media comprising a blend of medium sand and granular iron exhibit permeabilities dominated by the sand fraction up to 85% by weight iron. All samples with iron content below this amount displayed a hydraulic conductivity in the range of 44 to 61 m/d. Higher iron content leads to permeability increasingly dominated by the iron fraction.

Finally, it is concluded from this work that the laboratory-scale methods of grain size analysis and permeametry accurately determined the hydraulic conductivity of granular porous media in a scaled-up column of dimensions relevant to field applications and design work for the HRX Well. The practical relevance of this was demonstrated by using the measured values of K and gradient from the column test to estimate seepage velocities (v) (30 to 51cm/d) that were found to compare well to direct measurements of v using a PVP (38 to 60cm/d).

This result provides some of the first detailed, multi-scale evidence, not confounded by interferences due to reactive processes, that laboratory testing can accurately estimate field-scale K for engineered porous media relevant to remediation and other hydrogeological purposes. Additional work is needed to test still larger scale-ups of engineered media, such as reactive barriers. Further work is also needed to address the scaling complexities associated with reactive media such as mineral precipitation or gas formation. It must also be noted that these conclusions apply for engineered media similar in character to those studied here. Where media with substantially different grain size distributions are used (e.g., wood chips), additional preliminary testing should be conducted to re-assess which grain-size algorithms may be most suitable for those media.

2.6 Acknowledgements

This work was funded by DOD's ESTCP (ER-201631) through a subcontract to the University of Kansas by Arcadis. We acknowledge Trevor Osorno, Bryan Heyer, Matt Jones, and Billy Hodge for their assistance and helpful discussions.

2.7 References

Aguilar, J. R. 2013. Analysis of grain-size distribution and hydraulic conductivity for a variety of sediment types with application to wadi sediments. MSc Thesis submitted to King Abdullah University of Science and Technology, Thuwal, Kingdom of Saudi Arabia. doi: https://doi.org/10.25781/KAUST-A4P9F

American Society of Testing and Materials (ASTM). 1991. *Annual Book of ASTM Standards*, Designation D2434 – 68: Standard Test Method for Permeability of Granular Soils (Constant Head).

Aubertin, M., Bussiere, B., Chapuis, R. P. 1996. Hydraulic conductivity of homogenized tailings from hard rock mines. *Canadian Geotechnical Journal*, 33 (3):470-482. doi: https://doi.org/10.1139/t96-068

Barth, G. R, Hill, M. C., Illangasekare, T. H., Rajaram, H. 2001. Predictive modeling of flow and transport in a two-dimensional intermediate-scale, heterogeneous porous medium. *Water Resources Research*, 37 (10): 2503–2512. doi: https://doi.org/10.1029/2001WR000242

Białas, Z. 1966. O usrednianiu wspolczynnikow filtracji z zastosowaniem elektronicznej cyfrowej maszyny matematycznej [Averaging filter coefficients using digital electronic mathematical machines]. Przedsiebiorstwo Geologiczne we Wroclawiu, Warsaw, Poland, p 47–50.

Blohm, F. J. A. 2016. Determination of Hydraulic Conductivities through Grain Size Analysis.

M. Sc. Thesis submitted to Boston College, Boston, USA. http://hdl.handle.net/2345/bc-ir:106982

Bowles, M. W., Bentley, L. R., Hoyne, B., Thomas, D. A. 2000. In situ ground water remediation using the trench and gate system. *Ground Water*, 38 (2): 172-181. doi: https://doi.org/10.1111/j.1745-6584.2000.tb00328.x

Burbery, L. F., Abraham, P., Afrit, B. 2014. Determining the hydraulic properties of wood/gravel mixtures for use in denitrifying walls. *Journal of Hydrology*, 53 (1): 1-21. Available from https://www.jstor.org/stable/43945052.

Choo, H., Lee, W., Lee, C., Burns, S. E. 2018. Estimating Porosity and Particle Size for Hydraulic Conductivity of Binary Mixed Soils Containing Two Different-Sized Silica Particles. *Journal of Geotechnical and Geoenvironmental Engineering*, 144 (1): 04017104. doi: https://doi.org/10.1061/(ASCE)GT.1943-5606.0001802

Côté, J., Fillion, M-H., Konrad, J-M. 2011. Estimating Hydraulic and Thermal Conductivities of Crushed Granite Using Porosity and Equivalent Particle Size. *Journal of Geotechnical and Geoenvironmental Engineering*, 137 (9): 834-842. doi: https://doi.org/10.1061/(ASCE)GT.1943-5606.0000503

Critchley, K., Rudolph, D.L., Devlin, J.F., Schillig, P.C. 2014. Stimulating in situ denitrification in an aerobic, highly permeable municipal drinking water aquifer. *Journal of Contaminant Hydrology*, 171: 66–80. doi: https://doi.org/10.1016/j.jconhyd.2014.10.008

Darcy, H. 1856. *Les Fontaines Publiques de la Ville de Dijon [The Public Fountains of the City of Dijon]*. Dalmont, Paris.

Deo, O., Sumanasooriya, M., Neithalath N. 2010. Permeability Reduction in Pervious Concretes

due to Clogging: Experiments and Modeling. *Journal of Materials in Civil Engineering*, 22 (7): 741-751. doi: https://doi.org/10.1061/(ASCE)MT.1943-5533.0000079

Devlin, J. F. 2015. HydrogeoSieveXL : an Excel-based tool to estimate hydraulic conductivity from grain size analysis. *Hydrogeology Journal*, 23 (4), 837-844. doi: https://doi.org/10.1007/s10040-015-1255-0

Devlin, J. F., Barker, J. F. 1999. Field demonstration of permeable wall flushing for biostimulation of a shallow sandy aquifer. *Ground Water Monitoring and Remediation*, 19 (1): 75-83. doi: https://doi.org/10.1111/j.1745-6592.1999.tb00189.x

Devlin, J. F. 1994. Enhanced in situ biodegradation of carbon tetrachloride and trichloroethene using a permeable wall injection system. Ph. D. dissertation, Department of Earth Science, University of Waterloo, Waterloo, Ontario, Canada, 633 pp.

Divine, C. E., Roth, T., Crimi, M., DiMarco, A. C., Spurlin, M., Gillow, J., Leone, G. 2018a. The Horizontal Reactive Media Treatment Well (HRX Well®) for Passive In-Situ Remediation. *Groundwater Monitoring and Remediation*, 38 (1), 56-65. doi: https://doi.org/10.1111/gwmr.12252

Divine, C. E., Wright, J., Wang, J., McDonough, J., Kladias, M., Crimi, M., Nzeribe, B. N., Devlin, J. F., Lubrecht, M., Ombalski, D., Hodge, B., Voscott, H., Gerber, K. 2018b. The horizontal reactive media treatment well (HRX Well®) for passive in situ remediation: Design, implementation, and sustainability considerations. *Remediation*, 28 (4), 5-16. doi: https://doi.org/10.1002/rem.21571

Domga, R., Togue-Kamga , F., Noubactep, C., Tchatchueng, J-B. 2015. Discussing porosity loss of Fe0 packed water filters at ground level. *Chemical Engineering Journal*, 263: 127–134. doi: https://doi.org/10.1016/j.cej.2014.10.105

Driscoll, F. G. 1995. *Groundwater and wells*, second edition. Johnson Screens, St. Paul, Minnesota.

Fassman-Beck, E., Wang, S., Simcock, R., Liu, R. 2015. Assessing the Effects of Bioretention's Engineered Media Composition and Compaction on Hydraulic Conductivity and Water Holding Capacity, *Journal of Sustainable Water in the Built Environment*,1 (4): 04015003. doi: https://doi.org/10.1061/JSWBAY.0000799

Freeze, R. A., Cherry, J. A. 1979. *Groundwater*. Web version, http://hydrogeologistswithoutborders.org/wordpress/original-groundwater-by-freeze-and-cherry-1979-now-available-online/

Fronczyk, J., Pawluk, K. 2014. Hydraulic performance of zero-valent iron and nano-sized zero-valent iron permeable reactive barriers – laboratory test. *Annals of Warsaw University of Life Sciences – SGGW, Land Reclamation*, 46 (1): 33–42. doi: 10.2478/sggw-2014-0003

Gallardo, A. H., Marui, A. 2007. Hydraulic characteristics of sedimentary deposits at the J-PARC proton-accelerator, Japan. Earth Sciences Research Journal, 11 (2): 139-154. http://www2.lib.ku.edu/login?url=https://search.proquest.com/docview/1677640141?accountid=14556

Gierczak, R. F. D., Devlin, J. F., Rudolph, D. L. 2006. Combined use of field and laboratory testing to predict preferred flow paths in an heterogeneous aquifer. *Journal of Contaminant Hydrology*, 82(1-2): 75-98. doi: https://doi.org/10.1016/j.jconhyd.2005.09.002

Henderson, A. D. 2010. Solids formation and permeability reduction in zero -valent iron and iron sulfide media for permeable reactive barriers. Ph.D. dissertation, University of Michigan, Department of Environmental Engineering, UMI Number 3406477.

Hudak, P.F. 1994. Effective porosity of unconsolidated sand; Estimation and impact on capture zone geometry. *Environmental Geology*, 24: 140–143. doi: https://doi.org/10.1007/BF00767887

Istomina, V. S. 1957. *Filtration Stability of Soils*, Gosstroiizdat, Moscow.

Kasenow, M. 2002. *Determination of hydraulic conductivity from grain size analysis*. Water Resources, Highlands Ranch, CO.

Kempf, A., Divine, C. E., Leone, G., Holland, S., Mikac, J. 2013. Field performance of point velocity probes at a tidally influenced site. *Remediation*, 23 (1): 37-61. doi: https://doi.org/10.1002/rem.21337

Klute, A. 1965. Laboratory Measurement of Hydraulic Conductivity of Saturated Soil. In *Methods of Soil Analysis. Part 1. Physical and Mineralogical Properties, Including Statistics of Measurement and Sampling*, *Agronomy Monograph. 9.1* (13). Available from https://dl.sciencesocieties.org/publications/books/tocs/agronomymonogra/methodsofsoilana

Klute, A., Dirksen, C. 1986. Hydraulic conductivity and diffusivity: laboratory methods. In: Klute, A. (Ed.), *Methods of Soil Analysis, Part 1: Physical and Mineralogical Methods*, 2nd ed. Agronomy Monograph 9. ASA, Madison, WI, pp. 687–734.

Labaky, W., Devlin, J. F., Gillham, R. W. 2007. Probe for Measuring Groundwater Velocity at the Centimeter Scale. *Environmental Science & Technology,* 41 (24): 8453-8458. doi: 10.1021/es0716047

Liu, R., Fassman-Beck, E. 2016. Effect of Composition on Basic Properties of Engineered Media for Living Roofs and Bioretention. *Journal of Hydrologic Engineering*, 21 (6): 06016002. doi: https://doi.org/10.1061/(ASCE)HE.1943-5584.0001373

Mackay, D. M., Freyberg, D. L., Roberts, P. V. 1986. A natural gradient experiment on solute transport in a sand aquifer: 1. Approach and overview of plume movement. *Water Resources Research*, 22 (13): 2017-2029. doi: https://doi.org/10.1029/WR022i013p02017

Michette, M., Lorenz, R., Ziegert, C. 2017. Clay barriers for protecting historic buildings from ground moisture intrusion. *Heritage Science*, 5(31): 1-11. doi: https://doi.org/10.1186/s40494-017-0144-3

Mondal, P. K. 2004. Performance evaluation of fabric aided slow sand filter. University of Windsor (Canada), ProQuest Dissertations Publishing. MQ96402.

Morris, D. A., Johnson, A. I. 1967. Summary of hydrologic and physical Properties of rock and soil materials, as analyzed by the Hydrologic Laboratory of the U.S. Geological Survey, 1948-60. Geological Survey Water-Supply Paper 1839-D, U.S. Government Printing Office, Washington, 42 pp.

Nijp, J. J., Metselaar, K., Limpens, J., Gooren, H. P. A., *and* Van der Zee, S. E. A. T. M. 2017. A modification of the constant-head permeameter to measure saturated hydraulic conductivity of highly permeable media. *MethodsX,* 4, 134-142. doi: https://doi.org/10.1016/j.mex.2017.02.002

Page, B. J. 2016. Quantifying Hydraulic Conductivity in Mine Drainage Passive Treatment System Vertical Flow Bioreactors. Msc Thesis Submitted to University of Oklahoma, Norman, Oklahoma. Available from https://hdl.handle.net/11244/47069

Rice, J. D. 2007. A Study on the Long-Term Performance of Seepage Barriers in Dams Virginia Polytechnic Institute and State University, ProQuest Dissertations Publishing. DP19824.

Robertson, W. D., Ptacek, C. J., Brown, S. J. 2007. Geochemical and hydrogeological impacts of

a wood particle barrier treating nitrate and perchlorate in ground water. *Ground Water Monitoring and Remediation*, 27 (2): 85-95. doi: https://doi.org/10.1111/j.1745-6592.2007.00140.x

Rosas, J., Lopez, O., Missimer, T. M., Coulibaly, K. M., Dehwah, A. H. A., Sesler, K., Lujan, L. R., Mantilla, D. 2014. Determination of Hydraulic Conductivity from Grain-Size Distribution for Different Depositional Environments. *Groundwater*, 52 (3): 399-413. doi: https://doi.org/10.1111/gwat.12078

Scannell, L. W. 2016. An analysis of performance criteria of porous ceramic water filter production methods. Ph.D. dissertation, University at Buffalo, State University of New York, Dept., of Civil, Structural and Environmental Engineering.

Schipper, L. A., Barkle, G. F., Hadfield, J. C., Vojvodic-Vukovic, M., Burgess, C. P. 2004. Hydraulic constraints on the performance of a groundwater denitrification wall for nitrate removal from shallow groundwater. *Journal of Contaminant Hydrology*, 69: 263-279. doi: https://doi.org/10.1016/S0169-7722(03)00157-8

Schriever, W. 1930. Law of Flow for the Passage of a Gas-free Liquid through a Spherical-grain Sand. *Transactions of the AIME*, 86 (1): 329-336. doi: https://doi.org/10.2118/930329-G

Schultze-Makuch, D., Carlson, D. A., Cherkauer, D. S., Malik, P. 1999. Scale dependency of hydraulic conductivity in heterogeneous media. *Groundwater*, 37 (6): 904-919. doi: https://doi.org/10.1111/j.1745-6584.1999.tb01190.x

SERAS. 2003. Standard operating procedures, Determination of granular soil permeability (constant head), accessed at https://clu-in.org/download/ert/1842-r00.pdf, April 5, 2020, 14 pp.

Shepherd, R. G. 1989. Correlations of Permeability and Grain Size. *Groundwater*, 27 (5),

633-638. doi: https://doi.org/10.1111/j.1745-6584.1989.tb00476.x

Slichter, C. S. 1898. Theoretical investigations of the motion of ground waters. 19th annual report, US Geological Survey, Reston, VA, pp 295–384.

Song, J., Chen, X., Cheng, C. Wang, D., Lackey, S., Xu, Z. 2009. Feasibility of Grain-size Analysis for Determination of Vertical Hydraulic Conductivity of Streambeds. *Journal of Hydrology,* 375 (3-4), 428-437. doi: https://doi.org/10.1016/j.jhydrol.2009.06.043

St. Marseille, J. 1998. Design and operation of an on-site sewage treatment system using leaching chambers and a denitrifying sand filter. M.Sc. thesis, Queen's University (Canada), Department of Civil Engineering.

Van den Berg, E. H., de Vries, J. J. 2003. Influence of grain fabric and lamination on the anisotropy of hydraulic conductivity in unconsolidated dune sands. *Journal of Hydrology*, 283 (1-4): 244-266. doi: https://doi.org/10.1016/S0022-1694(03)00272-5

van Driel, P. W., Robertson, W. D., Merkley, L. C. 2006. Denitrification of agricultural drainage using wood-based reactors. *Transactions of the American Society of Agricultural Engineers,* 48 (1): 121–128. doi: 10.13031/2013.20391

Vienken, T., Dietrich, P. 2011. Field Evaluation of Methods for Determining Hydraulic Conductivity from Grain Size Data. *Journal of Hydrology,* 400 (1-2), 58-71. doi: https://doi.org/10.1016/j.jhydrol.2011.01.022

Vukovic M., Soro, A. 1992. *Determination of hydraulic conductivity of porous media from grain-size composition*. Water Resources Publications, Littleton, Colorado, USA.

Warith, M. A., Evgin, E., Benson, P. A. S. 2004. Suitability of shredded tires for use in landfill leachate collection systems. *Waste Management*, 24 (10): 967-979. doi: https://doi.org/10.1016/j.wasman.2004.08.004.

Zhang, J., Bruijnzeel, L. A., Quiñones, C. M., Tripoli, R., Asio, V. B., Van Meerveld, H. J. 2019. "Soil Physical Characteristics of a Degraded Tropical Grassland and a 'reforest': Implications for Runoff Generation." *Geoderma*, 333: 163-77. doi: https://doi.org/10.1016/j.geoderma.2018.07.022

Zhang, Y., Gillham, R.W. 2005. Effects of gas generation and precipitates on performance of Fe0 PRBs. *Ground Water*, 43 (1): 113-121. doi: https://doi.org/10.1111/j.1745-6584.2005.tb02290.x

3.0 Design, Testing, and Implementation of a Real-Time System for Monitoring Flow in HRX Wells

3.1 Abstract

The Horizontal Reactive Media Treatment Well (HRX Well®) is a technology recently introduced for aquifer remediation. It engineers a preferential flow pathway parallel to the direction of plume growth by emplacing a horizontal well, packed with a highly permeable reactive medium, into the aquifer. In a low permeability aquifer, the HRX Well collects and treats the water passively. Under passive operation, monitoring the flow through the well is necessary to ensure treatment is occurring in accordance with design specifications, and that the expected capture zone of the well is maintained. Point Velocity Probes (PVPs) were proposed to accomplish this task by placing them in cartridges within the HRX Well, a novel use for PVPs. The newness of the application required an assessment of the PVP, in particular for its performance in a confined setting with flow directed along the longitudinal axis of the probe. In addition, the detection of velocity variations due to gas generation from the reactive media within the HRX Well was investigated. A laboratory sand column, similar in size to the cartridges used in HRX Wells, was instrumented with PVPs of varying lengths (~ 2 to 17 cm) to assess the effects of friction at the fluid-solid (probe body) interface on velocity measurement bias. PVP length was found to impact velocity measurements insignificantly compared to the ±20% variation arising from packing variability. Gas produced from reactive media (mixture of sand and granular iron) was found to increase seepage velocity for fixed pumping rates. A field trial of the HRX Well demonstrated the viability and accuracy of PVPs in a full-scale system.

3.2 Introduction

Groundwater contamination in weakly permeable aquifers is a common problem worldwide. Passive treatment options are attractive when permeability is low because pumping is inefficient and sometimes impractical in these settings. A recent addition to the selection of technologies for *in situ* remediation, the Horizontal Reactive Media Treatment Well (HRX Well®), was developed to provide a cost-effective, passive, sustainable, and low-impact means of treating groundwater. The technology builds on the Permeable Reactive Barrier (PRB) concept (O'Hannesin and Gillham, 1998; Henderson and Demond, 2007; Obiri-Nyarko *et al.*, 2014; Divine *et al.*, 2018a), but potentially offering several advantages, including greater design control on hydraulic residence times, more efficient treatment media usage, the ability to install under buildings and other surface feature, smaller surface footprint, and lower lifecycle costs (e.g., Divine *et al.*, 2018; Divine *et al.*, 2020). HRX Wells function by creating a controlled preferential path for flow, within an aquifer of limited hydraulic conductivity (K), using a horizontal well packed with high permeability reactive media. The HRX Well is aligned with the primary direction of flow. Water is collected through a screened interval on the upgradient section of the well and discharged from a similarly screened downgradient section. Details of an example field design are available from Divine *et al.,* (2018b).

Central to the operation of the HRX Well is a predictable and verifiable flux of water entering and exiting the well. The flux determines both the amount of plume capture and the water residence times within the treatment media, which, in turn, governs the degree of water quality improvement from the system (Divine et al., 2018a). Point Velocity Probes (PVPs) are cost-effective devices capable of measuring seepage velocity in porous media. The measurements are made through the use of mini-tracer tests on the probe surface (Labaky *et al.*,

2007; Gibson and Devlin, 2018). With a reasonable estimate of effective porosity, PVP measurements can be converted to water flux through the HRX Well.

In this work, PVPs were installed for use in the first field scale HRX Well study at Vandenburg Air Force Base in California (Divine *et al*., 2018b). In advance of this deployment, novel design modifications and assessments were performed on the PVPs to verify their suitability for the HRX Well configuration and geometry. Specifically, the effects of the PVP shape and length, as well as the percent saturation of the reactive porous medium, were investigated for their influences on measured velocities. Since the HRX Well consisted of a packed cylinder with a limited diameter, there was concern that a PVP could potentially obstruct flow and negatively impact the capture of water by the HRX Well. In addition, the configuration of the PVP in the HRX Well required flow along the probe's main axis. Previous uses of the probe (Schillig *et al.,* 2011; Schillig *et al.*, 2016; Rønde *et al.,* 2017; Osorno et al., 2018) required only short distance of flow in contact with the probe for measurements to be made. In this application, the contact distance was comparatively longer. The possibility that the probe length could affect measurements due to drag on the probe surface therefore requires investigation.

A strength of the HRX Well technology is that the horizontal well can be packed with any of a variety of reactive media, which can be tailored to whatever pollutant(s) are targeted for treatment. The field test connected to this work was aimed at treating a chlorinated solvent plume containing trichloroethene (TCE), dichloroethene (DCE) isomers, and vinyl chloride (VC). A logical choice of porous medium in this case was one that incorporated granular iron. Treatability testing led to the final design utilizing a 35% by weight mixture of iron and coarse sand to reduce and dechlorinate the solvent compounds. Granular iron is well known for its

reactivity toward water, undergoing a reduction (of water) reaction to release hydrogen gas and hydroxyl ions (Reardon, 1995). The gas released can partially desaturate the medium, decreasing permeability (due to the pore space lost to gas bubbles). The hydroxyl ion is known to combine with dissolved ferrous iron to precipitate iron hydroxides and oxyhydroxides, and to drive the precipitation of carbonates by raising the solution pH (see Zhang and Gillham, 2005). The resulting loss of porosity to the mineral precipitates can also decrease permeability. Of these two effects, permeability loss due to gas production is expected to be the more pronounced over the short term, since gas production begins immediately upon wetting of the iron grains. Gas production rates tend to decline over time (Reardon, 1995). Mineral precipitation was less of a concern for the HRX Well demonstration project based on the results of site-specific treatability testing (Divine *et al.*, 2017), and the cartridge design on the system, which would allow exhausted media to be replaced as required. Therefore, this work emphasized the response of gas production on PVP measurements in the assessment of the probes.

The overall objectives of this study are to design a PVP probe suitable for deployment in the HRX Well system, assess the probe performance under conditions that might be expected in an HRX Well environment, and to assess the probe performance in a field demonstration of the HRX Well technology.

3.3 Methods

3.3.1 PVP testing

PVP tests were conducted within a 25 cm diameter, 30 cm long (Area = 491 cm^2) Plexiglas® column packed with a medium sand that had been identified as a possible packing material for HRX Well cartridges. The column was wet-packed in lifts around a PVP held in position with braces during the packing procedure. The cylindrical PVP was oriented with its

long axis aligned with the flow direction in the column. Two PVP designs were tested (See section 3.4.1, Figure 3.5a). The first was based on the Stream Bed Point Velocity Probe (SBPVP) shape (Cremeans and Devlin, 2017), with a short distance between the upgradient end of the 3-D printed probe head and the tracer detection arrays. For comparison, a second design that utilized less plastic and increased the separation distance between the end of the instrument and the detection array was realized. The second design had the possible advantage of circumventing possible interferences due to flow perturbations caused by flow redirection around the upgradient probe terminus. A centralizing tripod was also part of the original design but was replaced in the second design in favor of a less bulky centralizer placed distally from tracer detection array.

Flow was maintained through the column with a peristaltic pump with flow rates between 3.3 and 13.5 mL/min (Figure 3.1). Water was recirculated through the column from a 10 L high-density polyethylene carboy. The column was operated in a vertical orientation in most tests. The inlet port was located on the lower face and the effluent port on the top face. Each end plate was machined with 2 mm deep and 2 mm wide channels to equalize the hydraulic head. These channels were separated from the packed portion of the column by stainless steel screening that prevented sand from entering and clogging the channels. This construction ensured an even flow of water vertically upward through the column in all experiments. Manometers were located along the side of the column at distances of 6 cm and 21 cm from the inlet and were used to measure hydraulic head along the length of the column.

The PVP bodies and other supporting plastic pieces were generated on a U-Print 3-D printer (Osorno *et al.*, 2018; Walter and Devlin, 2017). PVP instrumentation was connected to a data logger in order to measure tracer breakthrough curves (BTC) from which velocity could be

calculated (Devlin *et al.*, 2009). PVP-measured velocity was compared to the seepage velocity calculated from measurements of column discharge, Q, and effective porosity, n_e,

$$v = \frac{Q}{An_e} \quad (1)$$

where A is the cross-sectional area of the column (L^2), v is the seepage velocity (L/T), and Q is the pumping rate (L^3/T). The total porosity of the medium grain sand was measured gravimetrically by packing pre-weighed sand in a 500 mL beaker, using the same technique for packed sand in the column, and then re-weighing the saturated medium. The mass difference was converted to water volume assuming a density of water of 1.00 gm/L. The cross-sectional area of the column available for flow was estimated by subtracting the cross-sectional area taken up by the PVP from the total cross-sectional area of the column.

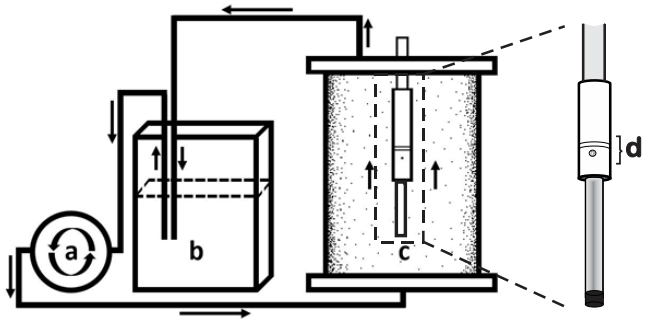

Figure 3.1: (a) Peristaltic pump recirculating flow from (b) a 10 L reservoir through a PVP Column filled with (c) porous media. (d) the detector array consisting of a tracer injection port and two detector wires. Arrows indicate the pathway of water flow within the closed system.

3.3.2 Modeling

Flow in a mock-HRX Well cartridge, consisting of a cylindrical sand-packed column with a centrally located PVP, was modeled using a 2-D iterative radial flow model, assuming a homogeneous and isotropic medium (Jacob, 1940),

$$\left(\frac{\partial^2 h}{\partial z^2}\right) + \frac{1}{r}\frac{\partial}{\partial r}\left(r\frac{\partial h}{\partial r}\right) = 0 \quad (2)$$

where, h is total hydraulic head (L), z is distance in the direction of flow, measured from base of the column (L), and r is the radial distance from the center axis of the column (L). In all simulations, constant head boundaries were established at the upgradient (bottom of the column) and down gradient (top of the column) ends of the model to establish desired flow rates, and water balances were calculated to verify mass was conserved. No-flow boundaries were established along the sides of the column and around the perimeter of the PVP, which was assumed to be solid, with no intrinsic porosity.

Equation 2 was solved using finite differences with a grid size of 0.1 cm by 0.1 cm for each PVP design, as well as a control case in which the PVP was absent. To examine the effect of PVP size on flow through the column, and associated seepage velocities, several simulations were performed with varying diameter PVPs. Upward velocity through the column, v_i, at each node was calculated using equation 3,

$$v_i = \left(\frac{K}{n_e}\right)\left(\frac{h_i - h_{i+1}}{\Delta z}\right) \quad (3)$$

where h_i is the hydraulic head (L) at a specified node within the model, h_{i+1} is the hydraulic head (L) in the node downgradient of h_i , Δz is the vertical grid spacing (L), and K is the hydraulic conductivity (L/T) of the porous medium filling the column.

Modeling of the field pilot HRX Well was performed for the purpose of estimating groundwater velocity inside the well, to compare against PVP measurements. Divine *et al.* (2018b) reported the results of three-dimensional simulations of the well for design purposes but assumed steady-state hydraulic conditions and therefore did not account for the range of hydraulic gradients that occurred during the field test and would have introduced variation into the PVP measurements. To address this added complexity, a simplified 2D finite difference flow model was executed, using the Dual Formulation equations given in Frind and Matanga (1985),

$$\frac{\partial}{\partial x}\left(T_{xx}\frac{\partial h}{\partial x}\right)+\frac{\partial}{\partial y}\left(T_{yy}\frac{\partial h}{\partial y}\right)=0 \tag{4}$$

$$\frac{\partial}{\partial x}\left(\frac{1}{T_{yy}}\frac{\partial \psi}{\partial x}\right)+\frac{\partial}{\partial y}\left(\frac{1}{T_{xx}}\frac{\partial \psi}{\partial y}\right)=0 \tag{5}$$

where, T refers to transmissivity (L^2/T), h is hydraulic head (L), representing potential, and ψ is the streamfunction (L^2/T). Constant head boundaries were used for the upgradient and downgradient ends of the modeled domain, and constant fluxes were defined ($q = 0$) for the sides. The streamfunction model was bounded according to equation 6,

$$\psi(\Gamma) = \psi_o(\Gamma_o) + \int_{\Gamma_o}^{\Gamma} \mathbf{q_o} \cdot \mathbf{n}\, d\Gamma \tag{6}$$

where, Γ refers to the boundary (L) an **n** is a normal unit vector. The node spacing was 15 m by 15 m with an overall model domain size of 450 m by 285 m.

3.3.3 Experimental evaluation of PVP length for its effect on velocity measurements

To provide insight on possible effects of an extended contact distance between water and the probe surface near the detector array of the PVP (Figure 3.1d), experiments were performed with five different probe lengths. As measured from the upgradient end of the 3-D printed plastic body to the injection port, these lengths were: 2.46 cm, 4.75 cm, 8.68 cm, 12.61 cm, and 16.54 cm. The 2.46 cm probe also had a smooth, 1.75 cm diameter metal rod on the upgradient side of the array, present in the design to support centralizers (note: the centralizers consisted of approximately 6 mm^2 gauge stainless steel wire with sufficient spring to hold the probe in place as the HRX cartridge was packed. Centralizers were not used in the laboratory tests for reasons of convenience). The narrower diameter (compared to the plastic of the probe) and smooth surface of the metal were assumed to contribute less drag to flow than the plastic parts.

Altogether, five flow rates (3.5, 5.5, 7.5, 9.5, and 11.5 mL/min) were applied to each of the five probes to generate five lines relating measured velocities with velocities expected from equation 1. All tests utilized a 0.3 mL injection of 1 g/L NaCl solution as the tracer. The tracer was introduced over a period of between 9 and 46 seconds with no notable effect on signal quality.

3.3.4 Effect of gas bubbles on measured velocity

The effect of gas production on PVP measurements was assessed in three ways. First, column tests were conducted with fully saturated sand. These were followed by draining of the

column, to residual saturation, and then re-saturation to entrap air in the pores. The medium sand used in this work was nearly identical to one reported by Li *et al.* (2013) (Figure 3.2A). That work generated drainage and imbibition curves for the sand, showing that the re-saturation level would be expected to be about 70% of full saturation (Figure 3.2B). The air trapped pore space this way was expected to be nearly uniform in its distribution, given the homogeneous and well-sorted nature of the sand (Figure 3.2A).

Second, the effect of gas production in an actual reactive medium was investigated by packing a column of identical dimensions with a mixture of 85% by weight granular iron (Connelly brand) and 15% coarse sand (see Cormican *et al.*, 2020). The column was instrumented with a PVP of design shown in Figure 3.5B. This medium is known to decompose water into hydrogen gas and hydroxyl ions (Reardon, 1996). The gas generation should, in principle, occur quite uniformly throughout the medium, at least initially. As it continues, bubbles may form and become mobilized. The desaturation of the medium could not be determined, but the effects of desaturation could be observed by changes to the seepage velocity, which were monitored with the PVP.

Finally, the influence of gas distributed *non-uniformly* near the detection array on – such as might occur if gas were inadvertently injected through the tracer injection port in a field test – was investigated. This case was examined in two separate tests: (1) a gas injection of approximately 1 mL and (2) a gas injection of approximately 4 mL were deliberately performed through the tracer injection port into an otherwise fully saturated column. The first injection was followed by repeated testing over seven days to assess the time required for the system to clear the gas from the detection array. The second injection was performed as a follow-up, to assess the effect of a larger gas injection volume.

All injections in this suite of tests were conducted using 0.1 mL of a tracer solution consisting of a 1 g/L NaCl solution, injected over a time period of between 13 and 18 seconds.

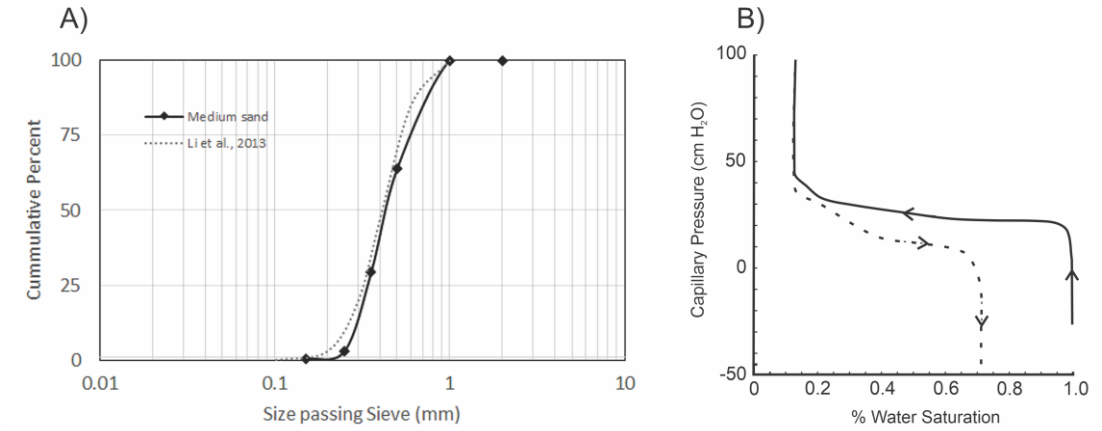

Figure 3.2: A) Grain size distribution of medium sand used in this work and that reported by Li et al. *(2013). B) Drainage and imbibition curves for the sand modified from Li* et al.*,* (*2013*).

3.3.5 Field Testing of PVPs in a full-scale HRX Well

The field-scale HRX Well was installed at the Vandenburg Air Force Base, California, in the summer of 2018. The horizontal well was about 172 m long, reaching a depth in the ground of about 7 m over the approximately 122 m long central, horizontal portion of the well. The total length of screen was about 50 m, and these sections were positioned on each end of the well where the casing rose to the surface. About 90 m of the central horizontal part of the well consisted of empty casing. The well was instrumented with sand-filled PVP cartridges, 1.5 m long and 0.25 m in diameter, at each end of the horizontal portion of the well (Figure 3.3), and seven 4.5 m long, 0.25 m diameter iron-containing reactive media cartridges were placed between them. All cartridges were sealed around their perimeters to prevent water from by-passing them and flowing between the casing and the cartridges. The aquifer in which the well was installed comprised a silty-clayey sediment that was found to have a median hydraulic

conductivity of about 0.11 m/day and a saturated thickness of approximately 3 m (Divine *et al*, 2020).

PVP testing was initiated in December, 2018, and continued until early 2020. Back-pressures were experienced in the tracer injection lines, requiring nominal injection volumes of up to 5 mL to ensure a measurable signal at the detectors. The tracer used was deionized water, which contrasted well in electrical conductance with the ambient groundwater (~9000 µS/cm). At least 30 minutes of background signal collection was gathered before each test. All data were collected on Campbell Scientific CR1000 dataloggers, as described by Devlin *et al.,* (2009), and the tracer signals were interpreted using VelProbePE software (Schillig, 2012).

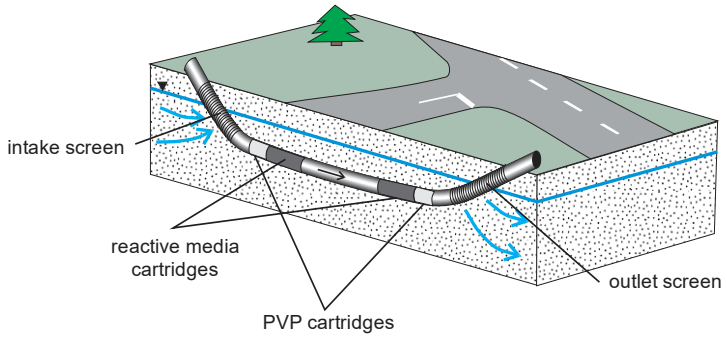

Figure 3.3: Schematic diagram of a passively operated HRX Well showing the location of the sand-packed PVP cartridges placed to monitor flow into and out of the closed treatment section of the well. Contaminated water enters the intake screen, and treated water exits through the outlet screen. Additional details are given in Divine et al. *(2020).*

3.4 Results and Discussion

3.4.1 Preliminary Modeling

Flow models conducted to assess the effects of probe size and shape were run with constant head boundaries at each end of a virtual cylindrical domain measuring 25 cm in diameter and 30 cm in length. A hydraulic gradient in the column of 0.0043 was assigned for the case where no PVP was present, corresponding to a discharge through the column of 5.5

mL/min. The porous medium was given a hydraulic conductivity of 40 m/day, selected on the basis of prior work reported by Cormican *et al.* (2020). Subsequent simulations, in which the various probe designs were evaluated, maintained the same discharge through the column. The effective porosity was assumed to be 0.3, based on velocity measurements reported below.

Simulations were conducted for a range of PVP diameters, including the two that were tested experimentally (Figure 3.5A-D). In no case did the simulations indicate a design-related bias to velocities on the probe surfaces where measurements were made. The only portions of the system where seepage velocity changed abruptly were at the tips of the probes and the immediate vicinities of some corners bounding the lower extension of the probe apparatus. Calculations (equation 7) of seepage velocity, *v*, using the Darcy equation, agreed well with the *v* values estimated using the flow model, lending confidence to the calculations (Figure 3.4).

$$v = -(A_c - A_{PVP})\frac{K}{n_e}\frac{\Delta H}{\Delta \ell} \tag{7}$$

where, $\Delta\ell$ is the column length (L), ΔH is the head drop over the column length (L), A_c is the cross-sectional area of the column (L^2), and A_{PVP} is the cross-sectional area of the PVP.

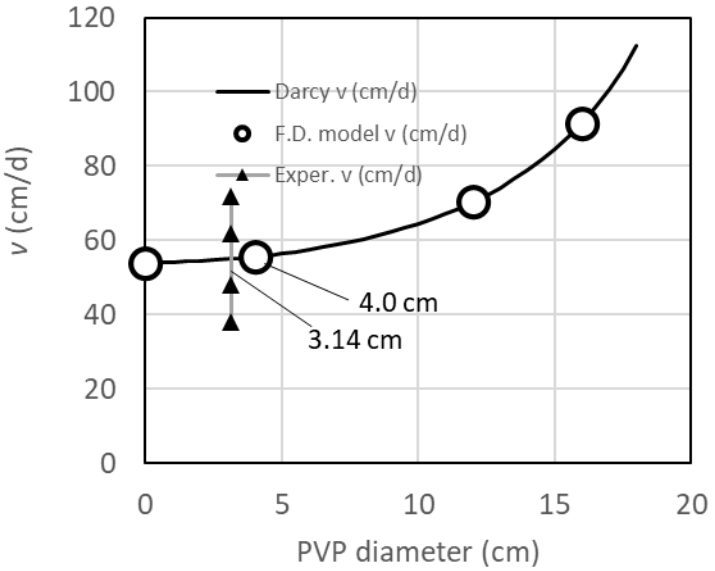

Figure 3.4: *Effect of PVP diameter on measurement accuracy. Simple Darcy calculations (Darcy v) and selected PVP radii in a radial finite difference flow model (F.D. Model v) show the measured velocity is a simple function of the net column cross-sectional area. Experimental results (Exper. v) show variation attributed to uncertainty in the effective porosity, which was found to vary ±20% from one packing to another.*

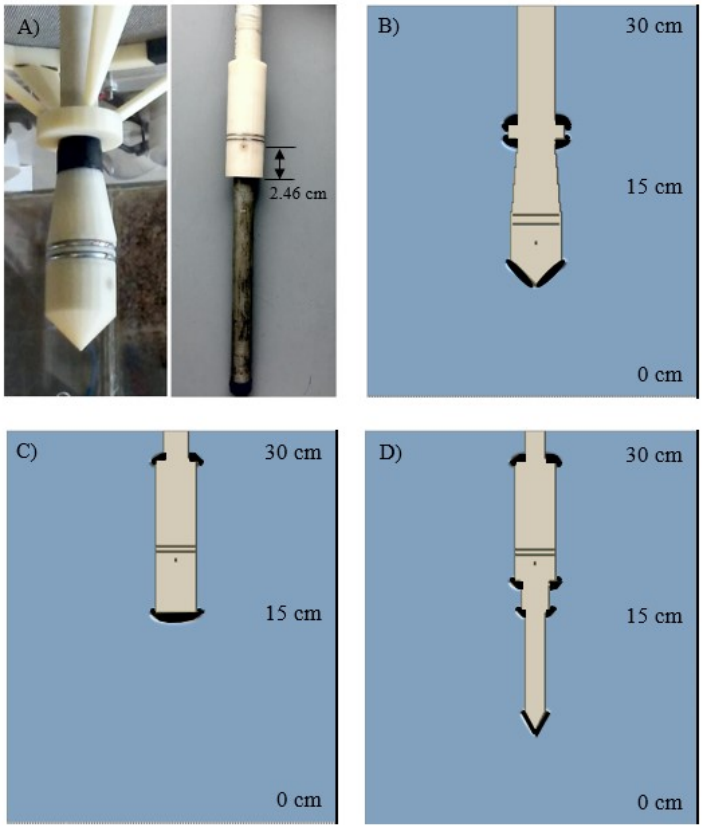

Figure 3.5: Model Simulations of vertical velocity distribution for various PVP probe designs within a sealed column. A) shows the PVP (left) used for saturation tests and 2.46 cm PVP (right) with metal rod attached used in the PVP length comparison tests. Note that the 2.46 cm measurement is from the injection port to the upgradient end of the probe. B) is a model simulation of the probe used in iron-sand mixture and sand-only column saturation tests. C) demonstrates a model of the 4.75 cm PVP used in the column length comparison tests. D) models flow around a PVP representative of the probe implemented in the HRX Well. The bottom of the column is the upgradient constant head boundary, while the top of the column is the downgradient constant head boundary, inducing an overall flow from bottom to top. The blue area filling the space around the probes is a region of uniform seepage velocity, within a range of ±0.1 cm/d. The dark areas near probe edges and termini show the regions where the velocity rapidly approaches zero as flow encounters solid obstructions that force flow redirection.

3.4.2 Effect of PVP Length on Velocity Measurements

Velocity measurements were conducted in four separate, sequential tests, with PVPs of increasing length. Each probe was packed in place with the medium sand described in Figure

3.2. Once packed, each probe was subjected to five flow rates, and the associated seepage velocities were measured. Flow rates were used in equation 1 to determine the expected seepage velocity. In each case, the relationship between expected and measured seepage velocities was found to be linear (Figure 3.6). It was expected that, if the contact distance between the water and instrument surface was a cause of bias to the velocity measurements, a trend of increasing bias should be associated with the increasing probe lengths – i.e., the slopes of the lines would change systematically, and in the same direction, as the sequence progressed. However, the variation in slopes was not found to vary systematically: the fastest flows were measured by the 12.61 cm and 2.46 cm PVPs, and the slowest flows were associated with the 8.68 cm and 16.54 cm long probes. The lack of a systematic trend in the lines indicates that factors other than the PVP lengths were responsible for the observed variation. The most likely factor responsible is the effective porosity.

The effective porosity is used in equation 1 to estimate seepage velocities expected for columns with and without probes in place. Variability in this parameter from one column packing to another is therefore a source of uncertainty in the analysis presented in Figure 6. Previously reported laboratory work indicated an uncertainty in estimated total porosity by the methods used here to be ±20% (Bowen *et al.,* 2012). Although effective porosity cannot be directly measured, it might be assumed to vary in proportion to total porosity. If so, then ±20% uncertainty may reasonably be expected to the effective porosity, and therefore to the equation 1 and 3 computations. The variabilities in the four lines in Figure 3. is almost entirely explained by this ±20% envelope of uncertainty. On this basis, the variability in these experiments is most likely due to porosity variations from column to column, due to packing differences. This finding does not rule out fluid drag on the PVP plastic surface as a contributor to bias. However,

it does show that such drag is a relatively minor concern. Nevertheless, the final design of the PVP for field use utilized a conservative 2.54 cm long probe to minimize bias that may not have been detected in these experiments.

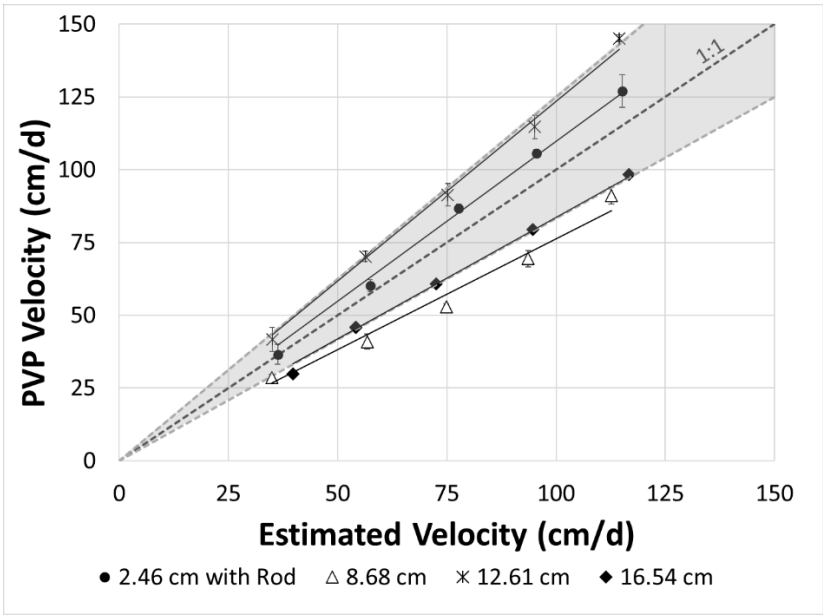

Figure 3.6: PVP velocity versus estimated velocity (based on discharge measurements from the column assuming an average effective porosity of 0.3) for multiple lengths of PVP. The standard deviation of PVP velocity repeat tests is shown for each of the points. Shading indicates a potential ±20% uncertainty due to porosity differences between packings.

3.4.3 Effect of Saturation on Measured Velocities

The experiments to investigate the effect of porous medium saturation on velocity measurements were conducted using the earliest probe design, shown in Figure 3.5A and B. Since the modeling work indicated no difference in performance between this design and the final one, the data presented here are considered to be applicable to both designs. Tests performed at the outset of this suite, in a freshly packed, fully saturated column (assuming a porosity of 0.33, which is comparable with the probe length series of tests reported above) found the measured velocities to be at the lower bound of the ±20% uncertainty envelope (Figure 3.7).

After draining and refilling the column, without altering the packing – so the total porosity, now the sum of water and air-filled porosity, remained constant – measured seepage velocities were found to increase. The amount of the increase could be fully explained by a decrease in saturated porosity, using equation 1, from 0.33 to 0.23, or 30%. This change in saturated porosity compares very well with expectations based on Figure 3.2B, which shows the highest degree of re-saturation expected for this type of sand is about 70%, i.e., a 30% decrease in saturated porosity from full saturation. This finding strongly supports the notion that the PVP could accurately detect water speed in uniformly unsaturated media and is consistent with experimental work reported by Berg and Gillham (2010) who applied PVPs to porous media above the water table.

It should be noted that in reactive media (as opposed to the non-reactive sand, discussed above), gas generation may continue until the bubbles become mobile and less uniformly distributed. The effect of this process on measured velocities was examined in sequential PVP measurements of velocity in a column packed with a mixture of sand and granular iron (Devlin *et al.,* 2018) (Figure 3.7). As might be expected in a column where gas production is ongoing and varying levels of saturation are experienced due to mobile bubbles, the measured seepage velocity in the column varied considerably. Nonetheless, in all tests the measured velocities exceeded the estimates from equation 1 by 20% or more (Figure 3.7). This finding is consistent with velocity enhancement due to porosity loss to gas, as documented in the more controlled re-saturated sand column, described above.

Air can be introduced and interfere with PVP tests inadvertently as a result of bubbles entering the tracer injection line. In this case, the gas is non-uniformly concentrated at the tracer injection port and detectors, potentially biasing velocity measurements. In each of two tests, the

first involving an approximate injection of 1 mL of air and the second 4.3 mL of air, a 15% decrease in experimental velocity was observed. The negative bias likely resulted from water redirected around the air-filled pores near the detectors. Essentially, the unsaturated volume of sand formed a zone of decreased permeability, slowing flow to the detectors. The similarity of results regardless of air injection volume suggests that similar amounts of air became trapped in the vicinity of the detection system in both tests. Excess air in the larger injection test was likely mobile enough to occupy volume in the sand removed from the probe surface. The velocity measurements returned to pre-air-injection conditions seven days after the air had been injected, suggesting that the air pockets had eventually become resaturated, perhaps by gas dissolution or mobilization (Figure 3.7).

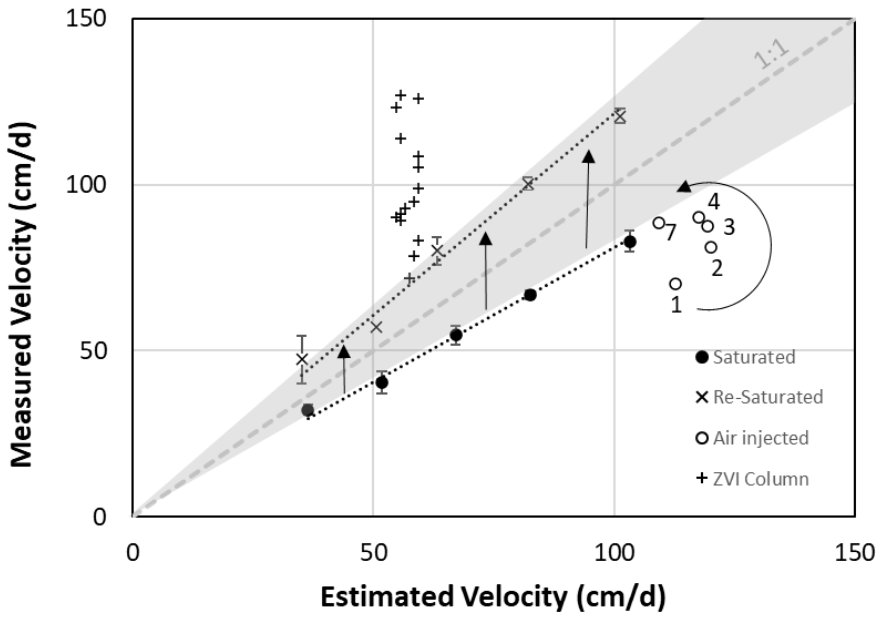

Figure 3.7: PVP velocity versus estimated velocity measured from column discharge (assuming a porosity of 0.33). "Saturated" represents the velocities based on a fully saturated column, "Air Injected" represents velocity measurements made for 7 days after injecting air through the PVP, and "Re-saturated" represents velocity measurements made within the re-saturated column. Arrows from the saturated column line to the re-saturated column line indicates the increase in measured PVP velocity after the column was re-saturated. Note that 7 days after air had been injected in the column, the velocity measurements returned to baseline. The curved arrow indicates the progression of days of measurements after injection of air. Point "1", one day after air was injected, displays the lowest PVP velocity. The points for the Saturated and Re-saturated tests represent average values from 3-10 repeat tests for each point. The standard deviation of PVP velocity repeat tests is shown for each of the points. Gas generated by granular (zero valent) iron (ZVI) resulted in variable increases to the measured seepage velocity in a similarly prepared column.

3.4.4 Field Testing in the HRX Well

A full-scale pilot test of the HRX Well system was installed at the Vandenberg Air Force Base in 2018. The aquifer was contaminated with trichloroethene, dichloroethene and vinyl chloride. It comprised approximately 3 m of unconsolidated alluvial materials that included fine-grained sands interspersed with discontinuous deposits of clay, silts, clayey sands, and silty sands designated as the Orcutt Formation sand of Late Pleistocene age (Dibblee 1989). The sediments exhibited an effective bulk hydraulic conductivity of 0.11 m/d. Further details of the site are available in Divine *et al.* (2020).

The HRX Well contained seven treatment media cartridges, each with 3 m of reactive material consisting of 35% granular iron and 65% coarse sand. The central portion of the HRX Well consisted of about 90 m of empty casing. The harmonic mean hydraulic conductivity of the overall well (K_{HRX}) was estimated to be about 270 m/d (Divine *et al.,* 2020).

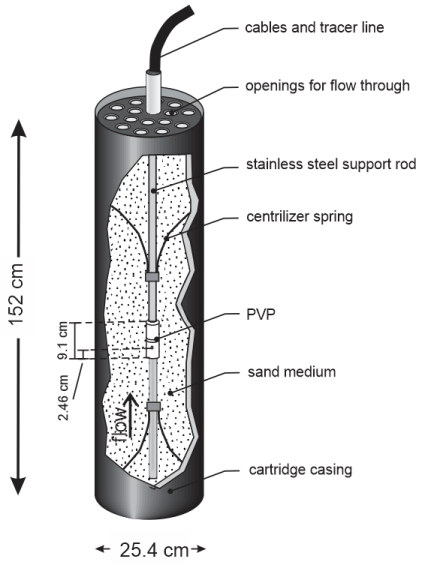

Figure 3.8: Cutaway view of PVP inside HRX Well outlet cartridge. The cartridge for the inlet side of the well has the PVP orientation reversed to accommodate flow in the other direction.

Using the information above, as outlined in Divine *et al.* (2018), the discharge through the HRX Well, and the seepage velocity in the treatment cartridges, were estimated from

$$Q_{HRX} = K_{HRX}(\pi r^2)i \qquad (8)$$

$$v = \frac{K_{HRX}i}{n_e} \qquad (9)$$

where, Q_{HRX} is the discharge through the HRX Well (L^3/T), n_e is the effective porosity (0.33 assumed) and i is the hydraulic gradient (dimensionless) inside the HRX Well (averaged over the entire length). Hydraulic head values in the inlet and outlet screens were approximated by using values obtained from standard monitoring wells located immediately next to the HRX Well screen. The hydraulic gradients were calculated using HydrogeoEstimatorXL software (Devlin and Schillig, 2017). This tool returns the hydraulic gradient in the direction of flow, which was, by design, aligned with HRX Well primary axis (within 16° ±14° in 6 of 8 water level surveys) but deviated more than 50° in 2 of the surveys. In all cases, the gradient used in equations 8 and 9 was the

component of the total gradient (from HydrogeoEstimatorXL) operating in the direction of the HRX Well (Figure 3.9).

The seepage velocity in the HRX Well was also estimated using numerical flow models. Divine *et al.* (2020) performed such simulations using MODFLOW, in which they assumed steady hydraulics and assigned constant flux boundary conditions. This resulted in a site-wide gradient of about 0.01 (this value is the approximate average gradient based on field measurements of hydraulic head at multiple wells over more than a decade), as well as hydraulic conductivities of 610 m/d for the HRX Well screen and open casing and 38.1 m/d for the treatment media and PVP sand cartridges. The results of the calculations from both Darcy and MODFLOW estimations of v were found to agree very well, with average v a little more than 2 m/d in both cases (Figure 3.9).

In order to facilitate numerical modeling that reflected the range of gradients encountered during this study, a two-dimensional flow model was developed and used to examine the relationship between the regional hydraulic gradient, the local gradient next to the HRX Well in the aquifer, the gradient within the HRX Well, and the seepage velocity in the media cartridges (Figure 3.). In all cases, these relationships were essentially linear. On this basis it was simple to convert field measurements of the hydraulic gradient near the HRX Well to seepage velocities in the media cartridges. Once again, the comparison with predictions from Darcy calculations and the single MODFLOW simulation were very good (Figure 3.9). It was against this background that the PVP measurements of velocity inside the HRX Well were interpreted.

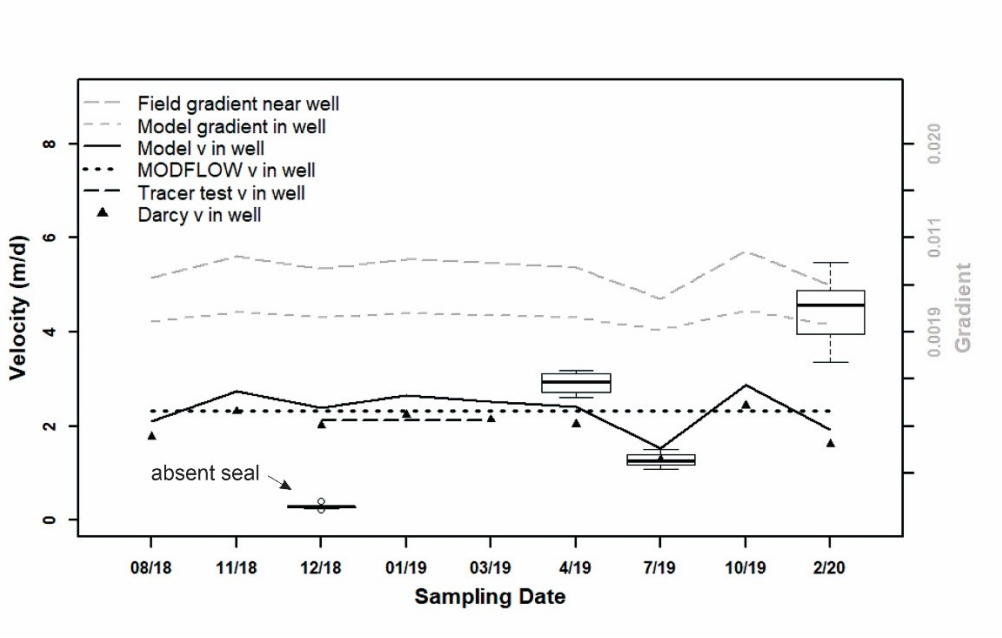

Figure 3.9: Linear velocity measured by PVPs within the HRX Well and site gradient for specific sampling dates. Boxplots indicate the measured velocities for each sampling date. The average velocity for December 2018 (12/18) is the average of 8 measurements taken at both the inlet and outlet PVP. Since the inlet PVP was no longer functional after installation of the seals, the 4 measurements taken in April 2019 (4/19), 3 measurements in July 2019 (7/19), and 5 measurements in February 2020 (2/20) represent averages from the outlet PVP only. The dashed line indicates the gradient at the site measured during the same week PVP tests were conducted.

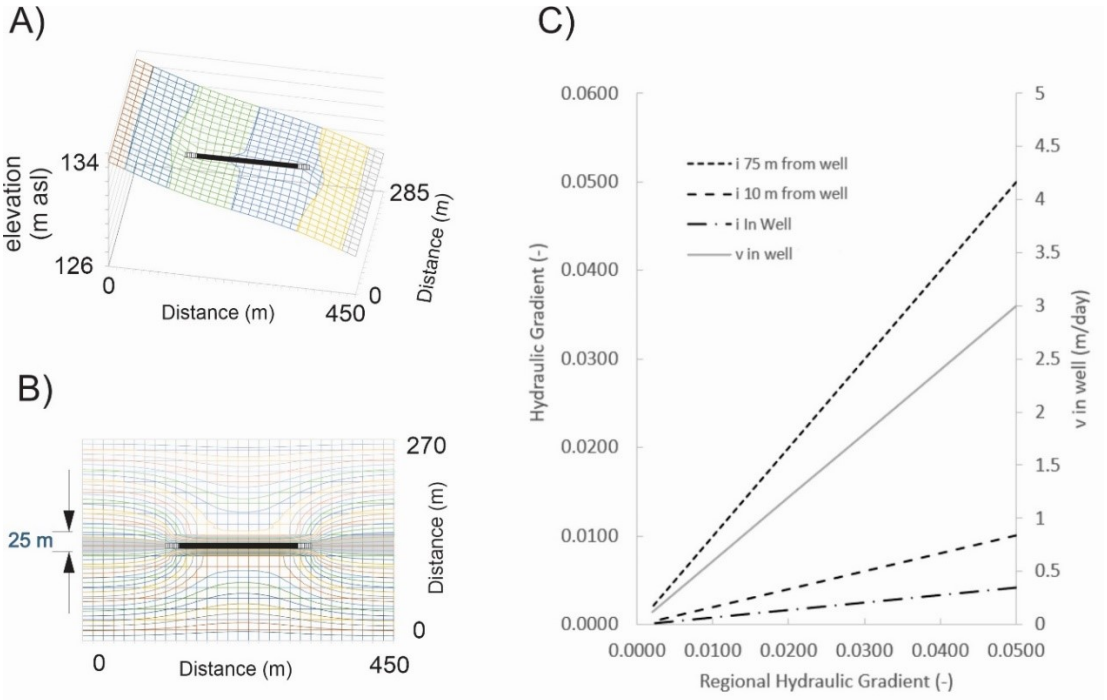

Figure 3.10: A) Visual representation of the effect of the HRX Well on the potentiometric surface during passive operation. B) Streamlines showing the extent of the capture zone for the HRX Well under conditions representative of those at the Vandenberg Air Force Base. The capture zone width of 25 m is comparable with the 15 m width calculated by Divine et al. (2018). The difference is attributed to the grid refinement. C) The 2D model indicated that the hydraulic gradient near and inside the HRX Well was, for practical purposes, linearly related to the regional gradient. This was also the case for the flow rate inside the well.

The first PVP velocity measurements were conducted in December, 2018, indicating seepage velocities averaging 0.29 m/d (n = 8 measurements over 3 days). As indicated inFigure 3.9, the expected velocity was almost an order of magnitude larger. A re-examination of the installation activities following this unexpected result revealed that the PVP cartridges had been installed without seals, which were required to prevent by-pass flow from occurring. It was hypothesized that these initial velocity measurements represented only a fraction of the total flow through the HRX Well, and, therefore, were biased low. Shortly thereafter, the PVP cartridges were retrofitted and the seals were properly established. The upgradient PVP unit was damaged during this process, so further tests were limited to the downgradient PVP. Measurements followed in April, 2019, (average v = 2.9 m/d), June, 2019, (average v =1.3 m/d), and February,

2020 (average v = 4.0 m/d). These results were in the range of the predicted values, suggesting that the HRX Well was functioning properly (Figure 3.9). The variation in PVP results across the different measurement dates suggests more transient hydraulic conditions were present than expected, and PVPs are able to measure short-term variations in flow conditions that represent maximum and minimum stresses on the treatment media.

The final tests, recorded in February, 2020, yielded velocities that were slightly greater than predictions based on the existing hydraulic gradients at the time. The reasons for this discrepancy are not known for certain. However, it could plausibly have arisen from one of three possible causes. First, the increase in velocity in February might be a result of decreased hydrogen gas production by the granular iron, and subsequent clearing of the pore space of bubbles. This could have caused a slight increase in K and slightly greater capture by the HRX Well without a noticeable change in hydraulic gradient. The needed change in K to effect the observed change in v is only about a factor of two, which is plausible. Second, it was noted during the PVP data interpretation that a large injection of tracer at the onset of the February, 2020, tests caused a significant slope to the signal baseline during the following tests. Although the subsequent tests all yielded signals that were clear and interpretable, some positive bias to the velocity estimates may have occurred during the baseline correction procedures. Third, water level measurement errors could have led to an erroneously low gradient, estimated to be 0.0064, compared to the site average, 0.0105. As a result, the predicted seepage velocity in the HRX Well would have been biased low. Using the site average gradient, seepage velocities are estimated to be in the range of 2.6 m/d to 3.3 m/d (Darcy and 2D model predictions, respectively), comparing more favorably with the PVP measurements.

3.5 Conclusion

Laboratory column studies and 2D-model simulations indicated an overall insensitivity of velocity measurements to PVP length and shape. On the other hand, the extent of the cartridge cross-sectional area taken up by the probe was determined to be a potentially significant factor for PVPs greater than 10 cm in diameter in a 25 cm diameter column (constituting about 16% of the internal column area), resulting in an increase cartridge seepage velocities. Both probes used in this study were less than 5 cm in diameter, suggesting minimal flow disturbance in the 25 cm HRX Well cartridges.

Alteration of seepage velocities with lower percent saturation in gas-producing reactive porous media was measurable using PVPs, with a 30% *increase* in measured velocity under controlled flow and uniformly distributed gas bubbles in the pores. It is noted that in an HRX Well under passive flow conditions, the decrease in percent saturation in granular iron reactive treatment media would see an alternate effect; measured seepage velocities would *decrease* due to a decrease in permeability as pores filled with gas were no longer available to conduct water. Lower weight percentages of granular iron media in the treatment cartridges, such as the 35wt.% of iron mixed with coarse sand at this field site, would help prevent drastic decreases in percent saturation by slowing gas production.

Field-site velocity measurements with a PVP in a full-scale HRX Well cartridge agreed well with predictions using two and three dimensional site flow models, with velocities measured throughout the year ranging from 1.3 to 4.0 m/d and model estimated values of 2.6 to 3.3 m/d. As a result of this study, PVPs have now been effectively implemented in the novel HRX Well cartridge environment and are performing the necessary flow monitoring through this passive treatment system.

3.6 References

Baveye, P., and Sposito, G. 1984. The Operational Significance of the Continuum Hypothesis in the Theory of Water Movement Through Soils and Aquifers. *Water Resources Research,* 20 (5): 521-530. doi: https://doi.org/10.1029/WR020i005p00521

Berg, S.J., Gillham, R.W. 2010. Studies of water velocity in the capillary fringe: the point velocity probe. *Ground Water*, 48 (1): 59-67. doi: https://doi.org/10.1111/j.1745-6584.2009.00606.x

Bowen, I.R., Devlin, J.F., Schillig, P.C. 2012. Design and testing of a convenient benchtop sandbox for controlled flow experiments. *Ground Water Monitoring and Remediation*, 32 (4): 87-91. doi: https://doi.org/10.1111/j.1745-6592.2012.01400.x

Cormican, A., Devlin, J.F. Divine, C. 2020. Grain Size Analysis and Permeametry for Estimating Hydraulic Conductivity In Engineered Porous Media. *Groundwater Monitoring and Remediation*, 40 (2): 65-72. doi: https://doi.org/10.1111/gwmr.12379

Cremeans, M., Devlin, J.F. 2017. Validation of a new device to quantify groundwater-surface water exchange. *Journal of Contaminant Hydrology*, 206: 75-80. doi: https://doi.org/10.1016/j.jconhyd.2017.08.005

Das, G. P. *Hydraulic Engineering: Fundamental Concepts*. 2016. Environmental Engineering Collection. Web.

Devlin, J.F., Hodge, B., Nzeribe, B.N., Crimi, M., Divine, C.E., Wright, J. 2018. The Horizontal Reactive Media Treatment Well (HRX Well®) for Passive In Situ Remediation: Selection of Treatment Medium and Velocity Probe TestingPoster presented at the SERDP/ESTCP Symposium, Washington, Nov. 27-29.

Devlin, J.F., Schillig, P.C. 2017. HydrogeoEstimatorXL: An Excel-based tool for estimating

hydraulic gradient magnitude and direction. Hydrogeology Journal, 25: 867-875. doi: 10.1007/s10040-016-1518-4.

Devlin, J. F., Tsoflias, G., McGlashan, M., Schillig, P. 2009. An Inexpensive Multilevel Array of Sensors for Direct Ground Water Velocity Measurement. *Ground Water Monitoring and Remediation,* 29 (v. 45), 73-77. doi: https://doi.org/10.1111/j.1745-6592.2009.01233.x

Dibblee, T.W., Jr. 1989. Geologic map of the Casmalia and Orcutt Quadrangles, Santa Barbara County, California: Dibblee Geological Foundation Map DF-24, scale 1:24,000.

Divine, C. E., Crimi, M., Devlin, J. F. 2017. Treatability test study report. Demonstration and Validation of the Horizontal Reactive Media Treatment Well (HRX Well®) for Managing Contaminant Plumes in Complex Geologic Environments. ESTCP Project 16 EB-ER1-046. 56 pp.

Divine, C. E., Crimi, M., Devlin, J. F. 2020. Final Report Demonstration and Validation of the Horizontal Reactive Media Treatment Well (HRX Well®) for Managing Contaminant Plumes in Complex Geologic Environments. ESTCP Project ER-201631. 72 pp.

Divine, C. E., Roth, T., Crimi, M., DiMarco, A. C., Spurlin, M., Gillow, J., Leone, G. 2018a. The Horizontal Reactive Media Treatment Well (HRX Well®) for Passive In-Situ Remediation. *Groundwater Monitoring and Remediation*, 38 (1), 56-65. doi: https://doi.org/10.1111/gwmr.12252

Divine, C. E., Wright, J., Wang, J., McDonough, J., Kladias, M., Crimi, M., Nzeribe, B. N., Devlin, J. F., Lubrecht, M., Ombalski, D., Hodge, B., Voscott, H., Gerber, K. 2018b. The horizontal reactive media treatment well (HRX Well®) for passive in situ remediation:

Design, implementation, and sustainability considerations. *Remediation*, 28 (4), 5-16. doi: https://doi.org/10.1002/rem.21571

Domenico, P. A., and Schwartz, F. W. *Physical and Chemical Hydrogeology*. New York, John Wiley and Sons, 1990.

Firdous, R., Devlin, J. F. 2014. Consideration of grain packing in granular iron treatability studies. *Journal of Contaminant Hydrology*, 164: 230-239. doi: http://dx.doi.org/10.1016/j.jconhyd.2014.05.014

Frind, E. O., Matanga, G. B. 1985. The dual formulation of flow for contaminant transport modeling 1. review of theory and accuracy aspects. *Water Resources Research*, 21 (2): 159-169. doi: https://doi.org/10.1029/WR021i002p00159

Gibson, B., Devlin, J.F. 2018. Laboratory validation of a point velocity probe for measuring horizontal flow from any direction. *Journal of Contaminant Hydrology*, 208: 10-16. doi: https://doi.org/10.1016/j.jconhyd.2017.10.005

Henderson, A. D., and Demond, A. H. 2007. Long-Term Performance of Zero-Valent Iron Permeable Reactive Barriers: A Critical Review. *Environmental Engineering Science*, 24 (4): 401-423. doi: https://doi.org/10.1089/ees.2006.0071

Jacob, C.E. 1940. On the flow of water in an elastic artesian aquifer. *Eos, Transactions American Geophysical Union*, 21 (2): 574-586. doi: https://doi.org/10.1029/TR021i002p00574

Kamolpornwijt, W., Liang, L.,West, O. R., Moline, G. R., Sullivan, A. B. 2003. Preferential flow path development and its influence on long-term PRB performance: column study. *Journal of Contaminant Hydrology*, 66(3-4): 161-178. doi: https://doi.org/10.1016/S0169-7722(03)00031-7

Labaky, W., Devlin, J. F., Gillham, R. W. 2007. Probe for Measuring Groundwater Velocity

at the Centimeter Scale. *Environmental Science & Technology,* 41 (24), 8453-8458. doi: 10.1021/es0716047

Li, Y., Flores, G., Xu, J.,Yue, W., Wang, Y., Luan, T., Gu, Q. 2013. Residual air saturation changes during consecutive drainage–imbibition cycles in an air–water fine sandy medium. *Journal of Hydrology*, 503: 77-88. doi: https://doi.org/10.1016/j.jhydrol.2013.08.050

Mioska, M. J. 2012. A Column Experiment for Groundwater Remediation Post-Mine Closure at the Wolverine Mine, Yukon. Masters Thesis through Royal Roads University, Victoria, BC.

Obiri-Nyarko, F., Grajales-Mesa, S. J., Malina, G. 2014. An overview of permeable reactive barriers for in situ sustainable groundwater remediation. *Chemosphere*, 111: 243-259. doi: https://doi.org/10.1016/j.chemosphere.2014.03.112

O'Hannesin, S. F., Gillham, R. W. 1998. Long-Term Performance of an In Situ "Iron Wall" for Remediation of VOCs. *Groundwater*, 36 (1): 164-170. doi: https://doi.org/10.1111/j.1745-6584.1998.tb01077.x

Osorno, T., Devlin, J.F. 2018. An in-well point velocity probe for the rapid characterization of groundwater velocity at the centimeter-scale. *Journal of Hydrology*, 557: 539-546. doi: https://doi.org/10.1016/j.jhydrol.2017.12.033

Parker, J. C. 1984. Analysis of Solute Transport in Column Tracer Studies. *Soil Science Society of America Journal*, 48 (4): 719-724. doi: https://doi.org/10.2136/sssaj1984.03615995004800040005x

Reardon, E. J. 1995. Anaerobic Corrosion of Granular Iron: Measurement and Interpretation of Hydrogen Evolution Rates. *Environmental Science and Technology*, 29(12): 2936-2945. doi: https://doi.org/10.1021/es00012a008

Rønde, V., McKnight, U.S., Sonne A.Th., Devlin, J.F., Bjerg, P.L. 2017. Contaminant mass discharge to streams: comparing direct groundwater velocity measurements and multi-level groundwater sampling with an in-stream approach. *Journal of Contaminant Hydrology*, 206: 43-54. doi: https://doi.org/10.1016/j.jconhyd.2017.09.010

Schillig, P.C. 2012. VelProbePE: An Automated Spreadsheet Program for Interpreting Point Velocity Probe Breakthrough Curves. *Computers & Geosciences*, 39: 161-170. doi: https://doi.org/10.1016/j.cageo.2011.06.007

Schillig, P. C., Devlin, J.F., McGlashan, M., Tsoflias, G., Roberts, J.A. 2011. Transient heterogeneity in an aquifer undergoing bioremediation of hydrocarbons. *Ground Water*, 49 (2): 184-196. doi: https://doi.org/10.1111/j.1745-6584.2010.00682.x

Schillig, P.C., Devlin, J.F., Rudolph, D. 2016. Upscaling point measurements of groundwater velocity for enhanced site characterization in a glacial outwash aquifer. *Groundwater*, 54 (3): 394-405. doi: https://doi.org/10.1111/gwat.12357

Walter, K., Devlin, J.F. 2017. Application of 3D printing to the manufacturing of groundwater velocity probes (PVPs). *Groundwater Monitoring and Remediation*, 37 (2): 71-77. doi: 10.1111/gwmr.12210.

Zhang, Y., Gillham, R.W. 2005. Effects of gas generation and precipitates on performance of Fe0 PRBs. *Ground Water*, 43 (1): 113-121. doi: https://doi.org/10.1111/j.1745-6584.2005.tb02290.x

4.0 Conclusions and Recommendations

4.1 Conclusions

4.1.1 Laboratory determination of K for Engineered Porous Media

From the work presented in this thesis, it is concluded that hydraulic conductivity of porous media sand samples can be accurately measured on the benchtop by either grain size analysis or permeametry when applied to the field-scale applications, provided the field media are packed in a comparable manner, i.e., the field media is engineered. When laboratory-measured *K* and column-measured hydraulic gradient were used to estimate seepage velocity in a field scale column (built to comparable radius of an HRX Well cartridge), these estimates (30 to 51 cm/d) matched very well with direct PVP seepage velocity measurements within the column (38 to 60 cm/d), indicating successful *K* estimation across sample sizes. The granular sandy porous media investigated in this thesis had d_{10} values no less than 0.2 mm (coarse sand fraction), and the grain size curves indicated a high degree of homogeneity in the samples for all mixtures of granular iron and sand media. This condition facilitated accurate hydraulic conductivity (*K*) estimation.

K estimates from 16 grain size analysis algorithms ranged over an order of magnitude, which is not uncommon for these methods. Based on comparisons between these grain size analysis estimates and those from constant-head permeametry and a field-scale HRX Well cartridge, it is concluded that the USBR, Slichter, and Shepherd grain size algorithms provide the most accurate estimates for the sand under study. This conclusion is independently corroborated by published work that reported similar findings for similar sandy media (Song *et al.*, 2009; Blohm, 2016).

Mixtures of porous media are used in a variety of applications, including the formulation of reactive porous media for *in situ* groundwater remediation. It is concluded on the basis of grain size analysis and permeametry that in mixtures of medium sand and granular iron, the K of a mixture is not discernable from that of the medium sand alone until the iron content exceeds 85wt.% . Further work is needed to extend this finding to mixtures of media with more greatly contrasting grain size distributions.

4.1.2 Application of PVPs in Granular media-filled cartridges

On the basis of modeling and laboratory experimentation performed as part of this work, it is concluded that the performance of a PVP, adapted for us in a cylindrical container, is insensitive to the contact length in the direction of flow between the water and probe surface (over a range of 2 to 17 cm) or minor differences in probe shape. The length of PVP along the flow path on the longitudinal axis of the probe did not significantly alter flow, compared to a ±20% variability in porosity between column packings for different lengths of probe (Bowen *et al.*, 2012). Of greater concern is the proportion of cross-sectional area the PVP occupies in the cylinder. No practical effects on flow were noted for probes that occupied less than one third of the cylinder area.

Gas production, like the presence of the probe itself, can occupy space otherwise available for water flow. In reactive porous media, processes including gas production or mineral precipitation can dynamically alter the effective porosity. The experimental work conducted in this thesis demonstrated that the changes to flow due to desaturation by gas was detectable and quantifiable with the PVP technology. Under conditions of constant pumping, the reduction in effective porosity following the complete drainage and re-saturation of a medium-sand packed column was estimated to be 30% of the pore volume. Seepage velocities measured

in the saturated and re-saturated columns were also about 30% apart, with the unsaturated column exhibiting the *higher* velocity values, in keeping with expectations for the case of constant discharge and diminishing cross-sectional area for flow. It is important to note that in the field application of an HRX Well (or other *in situ* reactive medium systems), the reduction in effective porosity by gas accumulation would manifest itself in the form of *reduced* velocity measurements, due to a lower K and the possibility for water to be diverted around the well rather than passing through it.

Field measurements of seepage velocity within the HRX Well (1.3 to 4.0 m/d, depending on the time of year) indicated seepage velocities within the expected range (2.6 to 3.3 m/d). Moreover, the PVP detected abnormally low flow rates when a seal was omitted during the installation of the HRX Well. Expected flow rates were only detected after the seal was retrofitted. It is concluded from this that the PVP functioned properly in the field setting and the probe served as a rapid indicator of HRX Well performance.

4.1.3 Broader Significance of this Research

In addition to the contributions of this research specific to the HRX Well technology, several outcomes may be relevant to other technological applications and broader scientific questions. First, the demonstration in Chapter 2 that grain size analysis and permeametry can accurately characterize sandy media for scaled up applications fills a gap in the literature. Previously, most studies connected with this issue presume beforehand that the benchtop tests are accurate, without actually verifying the assumption. In many cases the assumption was shown to be false, or the studies were too limited to draw conclusions about its validity. Studies with reactive media were commonly confounded by interfering processes related to the chemical reactions involved.

The demonstration that mixed sandy porous media take on the hydraulic properties of the finer grained medium up to a mixture of 85% wt. coarse, 15% wt. fine is of value to any application that relies on multiple porous media blends. For groundwater remediation, reactive porous media is one example of this. In engineering, this work may have relevance for filtration work or fixed bed reactors.

The application of simple two-dimensional models to address three-dimensional problems is subject to misleading outcomes in many cases. However, this work has demonstrated two cases – modeling linear flow through a cylinder with a radial flow model and the HRX Well system with a two dimensional finite difference model – in which the absence of the third dimension greatly simplified the calculations without compromising the needed accuracy of the simulations. This finding has value for other, similarly configured studies.

Finally, PVP technology is a relatively new addition to the toolbox of methods available to hydrogeologists interested in flow system characterization. This study provides the fourth adaptation (after the PVP, IWPVP and SBPVP) of point velocity probes for measuring seepage velocity directly. The demonstrated broad applicability of this technology has value well beyond this immediate research.

4.2 Recommendations

Further work is needed to expand and verify the multi-scale application of laboratory K measurements for other engineered granular porous media, such as filter packs, wood chips, zeolite, and other common media used in reactive barrier systems. A major consideration for future work is the importance of grain size similarity for the successful prediction of hydraulic properties of mixtures. In addition, these methods also should be evaluated for their accuracy

vis-à-vis field applications with scales larger than the HRX Well, such as permeable reactive barriers.

With regard to reactive media, granular iron in this case, the tracking of declines in *K* due to mineral precipitation and gas production over long time periods (years) by direct velocity measurement has yet to be demonstrated. This kind of study would be facilitated by the automation of the PVP hardware.

In order to better quantify the effects of porous medium de-saturation on seepage velocities, further work is needed with columns of varying degrees of desaturation. This might be accomplished with a series of columns containing media of different grain sizes, tested at full saturation and at residual saturation. Alternatively, a single medium might be tested for varying degrees of de-saturation. The amount of de-saturation could be assessed gravimetrically or with advanced instruments such as NMR. Additionally, an interesting follow-up to this research would be to conduct laboratory column tests using the specific 35wt.% granular iron and coarse sand mixture to analyze how much gas is really being produced. The following tests could be conducted: (1) water velocity in the laboratory iron-sand mixture column could be measured to help predict the effect of gas production on measurements, and (2) water velocity in multiple long-term columns side-by-side (containing either deionized water or field site water without the contaminants) could be measured to predict what is occurring at the field site. Another interesting follow-up to this research would be to generate a reducing environment, as seen in the field HRX Well, in the granular iron column tests to compare how this would impact overall gas production and velocity measurements (note, column experiments in this thesis were done in open-air conditions and without any reactive media).

Lastly, direct measurements of regional gradient at the HRX Well would be beneficial for estimating overall capture width from PVP seepage velocities, instead of extrapolating a regional gradient from gradients measured adjacent to the HRX Well. Further tests could be conducted at different times of the year in the HRX Well with the PVP, coupled with measurements of a more regional hydraulic gradient not impacted by the well, to get a better idea of how much of the aquifer is being treated by the HRX Well.

4.3 References

Blohm, F. J. A. 2016. Determination of Hydraulic Conductivities through Grain Size Analysis. M. Sc. Thesis submitted to Boston College, Boston, USA. http://hdl.handle.net/2345/bc-ir:106982

Bowen, I. R., Devlin, J. F., Schillig, P. C. 2012. Design and Testing of a Convenient Benchtop Sandbox for Controlled Flow Experiments. *Groundwater Monitoring and Remediation*, 32 (4): 87-91. doi: https://doi-org.www2.lib.ku.edu/10.1111/j.1745-6592.2012.01400.x

Song, J., Chen, X., Cheng, C. Wang, D., Lackey, S., Xu, Z. 2009. Feasibility of Grain-size Analysis for Determination of Vertical Hydraulic Conductivity of Streambeds. *Journal of Hydrology,* 375 (3-4), 428-437. doi: https://doi.org/10.1016/j.jhydrol.2009.06.043